CALCULATION OF FRACTIONAL FLOW RESERVE (FFR) USING CT ANGIOGRAPHY IMAGES

Author

SHEIKH ARSLAN WAQAR

Registration Number

00000170605

Supervisor

DR. ZARTASHA MUSTANSAR

DEPARTMENT OF BIOMEDICAL ENGINEERING & SCIENCES

SCHOOL OF MECHANICAL & MANUFACTURING ENGINEERING

NATIONAL UNIVERSITY OF SCIENCES AND TECHNOLOGY

ISLAMABAD

APRIL 2020

Calculation of Fractional Flow Reserve (FFR) using CT Angiography Images

Author

Sheikh Arslan Waqar

Registration Number

00000170605

A thesis submitted in partial fulfilment of the requirements for the degree of

MS Biomedical Engineering

Thesis Supervisor:

Dr. Zartasha Mustansar

Thesis Supervisor's Signature: ____________________________________

DEPARTMENT OF BIOMEDICAL ENGINEERING & SCIENCES

SCHOOL OF MECHANICAL & MANUFACTURING ENGINEERING

NATIONAL UNIVERSITY OF SCIENCES AND TECHNOLOGY

ISLAMABAD

APRIL 2020

Thesis Acceptance Certificate

It is certified that the final copy of MS Thesis written by **Sheikh Arslan Waqar** *(Registration No. 00000170605)*, of SMME (School of Mechanical & Manufacturing Engineering) has been vetted by undersigned, found complete in all respects as per NUST statutes / regulations, is free of plagiarism, errors and mistakes and is accepted as partial fulfilment for award of MS/MPhil Degree. It is further certified that necessary amendments as pointed out by GEC members of the scholar have also been incorporated in this dissertation.

Signature: Zartasha ____________________

Name of Supervisor: Dr. Zartasha Mustansar

Date: 7th August, 2020

Signature (HOD):____________________

Date: ____________________

Signature (Principal):____________________

Date: ____________________

FORM TH-4

National University of Sciences & Technology

MASTER THESIS WORK

We hereby recommend that the dissertation prepared under our supervision by: **Sheikh Arslan Waqar** (Registration # 00000170605) Titled: "**Calculation of Fractional Flow Reserve (FFR) using CT Angiography Images**" be accepted in partial fulfilment of the requirements for the award of MS degree. GRADE: A

Examination Committee Members

1. Name: Dr. Syed Omer Gilani Signature:

2. Name: Engr. Sikander Hayat Mirza Signature:

Co-Supervisor's name: Dr. Muhammad Nabeel Anwar Signature:

Supervisor's name: Dr. Zartasha Mustansar Signature: Zartasha

Date: 7th August, 2020

Head of Department Date

COUNTERSINGED

Date: ________

Dean/Principal

Declaration

I certify that this research work titled "*Calculation of Fractional Flow Reserve (FFR) using CT Angiography images"* is my own work. The work has not been presented elsewhere for assessment. The material that has been used from other sources it has been properly acknowledged/referred.

Signature of Student

Sheikh Arslan Waqar

00000170605

Plagiarism Certificate (Turnitin Report)

This thesis has been checked for Plagiarism. Turnitin report endorsed by Supervisor is attached.

Signature of Student

Sheikh Arslan Waqar

00000170605

Signature of Supervisor

Dr. Zartasha Mustansar

Copyright Statement

- Copyright in text of this thesis rests with the student author. Copies (by any process) either in full, or of extracts, may be made only in accordance with instructions given by the author and lodged in the Library of NUST School of Mechanical & Manufacturing Engineering (SMME). Details may be obtained by the Librarian. This page must form part of any such copies made. Further copies (by any process) may not be made without the permission (in writing) of the author.
- The ownership of any intellectual property rights which may be described in this thesis is vested in NUST School of Mechanical & Manufacturing Engineering, subject to any prior agreement to the contrary, and may not be made available for use by third parties without the written permission of the SMME, which will prescribe the terms and conditions of any such agreement.
- Further information on the conditions under which disclosures and exploitation may take place is available from the Library of NUST School of Mechanical & Manufacturing Engineering, Islamabad.

Acknowledgements

First of all, I want to thank to my creator, the most gracious and the most merciful almighty ALLAH who has blessed me with an easier life, guided me through the darkest of times and protected me from countless hardships. He has graced my life with opportunities which were neither in my hands nor in any human's hands and in my opinion, had I never deserved them at all. Without his countless blessings, I would not have been the way I am today.

I am profusely thankful to my beloved parents who trust me with everything and shaped me in the best possible way they could do. I am thankful to them for their unparalleled love and continuous support. I am also thankful to my siblings who are always there for me at every step of my life. I am thankful to all my friends and family for having a blind faith in me.

I want to specially thank to my supervisor Dr. Zartasha Mustansar who had encouraged me to work on this thesis and from writing to presentation, without her guidance, it would not have been possible for me to finish it in an elegant way. Without her assistance in computational resource, implementation of computational models and a continuous feedback; the outcome of this project would certainly had been of lower quality.

I also like to express my deepest gratitude to my co-supervisor Dr. Muhammad Nabeel Anwar for being supportive throughout this project. I am thankful to him for his general guidance, continuously coming with suggestions for my work and responding on my urgent requests, despite of his busy schedule and workload. I also want to thank to Engr. Sikander Hayat Mirza for his cooperation in the thesis regarding the patient data.

I want to thank Dr. Umar Ansari who guided me whenever I asked for any kind of help and Dr. Adeeb Shehzad and Dr. Syed Omer Gillani who both had been very kind to me during my time here.

I want to especially thank to Dr. Nauman Naseer from Bahria International Hospital, Dr. Mehmood Zeb from Shifa International Hospital and Dr. Muhammad Saleem Khan, Dr. Waqar Ahmed and Dr. Akram from Kulsum International Hospital. Without their guidance it had been impossible to deal with the physiology and anatomy of cardiovascular systems.

I am thankful to all the members of Human Systems Lab including my seniors Ahmed Raza, Atif Sultan, Saad Habib, Azeem Alvi, Areena Khan, Zaeem Hadi, Ayesha Ambreen, Amna Malik, Kinza Waqar, Namra Afzal, Izzat Fatima, Zaid Ahsan Shah and my fellows Azmat Ullah, Aftab Ullah, Ahmed Subhani, Anisa Tahir, Hunza Hayat and Saroosh Bilal for helping me in their own ways and pushing me to achieve my potential and simply being there without and personal gains or requirements. I am also thankful to those senior members of HSL especially Amnah Mahroo who are continuously sharing further opportunities and guiding their juniors for PhDs. I feel lucky to have these humble people in my life.

I would also like to thank the staff in SMME specially Hafiz Azhar in CVML lab, Farrukh and Zubair in exam cell and PAs Jamil and Suleman, for being nice and making things easier for me here despite being busy with their own work.

In the end, I wish all people that I mentioned happiness in their lives, and I apologize to anyone I missed. Every person I met, mentioned or not, has been a learning experience for me. May Allah grant them whatever they wish and that is good for them. May Allah ease their hardships, help them in their problems and guide them to the right path.

Sheikh Arslan Waqar

Dedicated to the future of Computational Fluid Dynamics (CFD) in Biomechanics & Biomedical Engineering

Abstract

Fractional flow reserve (FFR) is a novel and clinically useful technique used in coronary catheterization to measure pressure differences across coronary artery stenosis (narrowing, usually due to atherosclerosis). It is considered now-a-days, as a gold standard to assess whether any particular stenosis is responsible for inducible ischemia. Angiography can be used additionally for the visual evaluation of the inner diameter of a vessel. In ischemic heart disease, identification of narrowing of vessel for potential lesion is not straightforward and consumes a lot of time. Fractional flow reserve on the contrary, provides a functional evaluation by measuring the pressure decline caused by a vessel narrowing.

The main objective of the study is to calculate FFR non-invasively to help in the prognosis of pressure drop of blood flow across stenosis. This will overcome the previously established invasive procedures of calculating FFR normally done in cardiac catheterisation. The exceptionality of this work undertakes modelling of non-Newtonian pulsatile blood flow. Present work incorporates the modelling of 3D coronary artery using CT Angiography DICOM images and simulation of non-Newtonian, pulsatile and non-pulsatile blood flows using computational fluid dynamics (CFD).

The results show that the transient, non-Newtonian pulsatile blood flows give more accurate results to mimic invasive FFR as compared to steady and transient non-pulsatile blood flows. The correlation of results obtained from this study are 100% in agreement with those obtained from invasive Angiography based FFR. We hope this non-invasive method will provide new pathway as a tool for diagnosis and evaluation of the narrowing caused by stenosis is coronary arteries.

Key Words: *Cardiovascular Diseases (CVD), Coronary Artery Diseases (CAD), Computational Fluid Dynamics (CFD), Finite Element Method (FEM), Computed Tomography Angiography (CTA), Digital Imaging and Communications in Medicine (DICOM)*

Table of Contents

List of Figures

List of Tables

Acronyms

CA	Coronary Artery
CAD	Coronary Artery Disease
CFD	Computational Fluid Dynamics
CT	Computed Tomography
CO	Cardiac Output
CVD	Cardiovascular Disease
FEM	Finite Element Method
FFR	Fractional Flow Reserve
FFR_{CT}	Computational Fractional Flow Reserve
ICA	Invasive Coronary Angiography
LAD	Left Anterior Descending Coronary Artery
LCA	Left Coronary Artery

LCX	Left Circumflex Coronary Artery
LM	Left Main Coronary Artery
LV	Left Ventricle
MAP	Mean Arterial Blood Pressure
N-S	Navier-Stokes Equations
PDE	Partial Differential Equations
PP	Pulse Pressure
RCA	Right Coronary Artery
SBP	Systolic Blood Pressure

CHAPTER 1. INTRODUCTION

Cardiovascular diseases (CVD) is the most alarming healthcare challenge in the world. It has the highest mortality rate globally, with approximately 17 million deaths each year, which is 31% of all deaths worldwide and it is expected that these numbers will increase substantially in the future [1]. Almost half of them are primarily attributed to coronary artery disease (CAD) [2] which is characterized by plaque build-up within these arteries. A novel and potentially useful technique which measures pressure differences across a stenosis[1] is the calculation of fractional flow reserve (FFR) which is recognised as the main practice for the examination of CAD. Although FFR has been found much better as compared to its substitutes in both cost [3, 4] and reliability [5-7], its efficiency and success rate has been found to be still disputable [8].

1.1. Thesis Objective

This thesis aims at the calculation of FFR with the main objective being:

- Calculation of Fractional Flow Reserve (FFR) using CT Angiography images

The following objectives are expected to be met in order to achieve our main objective:

- Develop a methodology for the calculation of FFR non-invasively at low computational expense
- Validate computational model of the patient specific coronary flows
- Develop pulsatile and non-pulsatile flows
- Simulate steady and transient blood flow
- compare the results

1.2. Motivation

Being a costly and sometimes an unnecessary procedure for the evaluation of pressure drop across a stenosis, invasive procedure of the calculation of FFR has proven to be a headache for

[1] Stenosis: It is a narrowing section in an artery which causes a pressure drop of the blood flow

both the doctors and patients.

In a country like Pakistan where basic health facilities are compromised, coronary heart diseases need to be treated on an immediate basis. Moreover, long waiting lists in government hospitals can delay the procedure by 3 to 4 months and not everyone can afford the expenses of private hospitals.

In the evolving field of personalized medicine, modern and unorthodox methods taking the advantage of the evolution in artificial intelligence, medical imaging and computational fluid dynamics are some generally believed to be the most challenging techniques to measure FFR. Non-invasive calculation of FFR and CAD assessment depending upon physical calculations, is about to revamping the existing procedures of clinical assessment by using modern techniques in simulating the blood flow on patient-specific models.

My personal motivation for opting this topic for research is the use of the field of computational fluid dynamics (CFD) in personalised healthcare. This technique will help to understand the vascular system in a much better and more efficient way which in turn will help to revolutionize the field of biomechanics.

The developed method will serve as a post-processing tool for the CT scans. Hence, without going through a needless invasive procedure, the doctors will easily be able to suggest to the patients an effective treatment plan like coronary angioplasty, stenting or a heart-bypass.

1.3. Outline

The rest of the thesis is organised in six chapters. CHAPTER 2 represents the different theoretical topics from different fields of the relevance. CHAPTER 3 describes the methodology employed in the development and simulation of computational models. The results obtained from the CFD simulations are presented in CHAPTER 4. CHAPTER 5 explains the comprehensive discussion on methods and results. Finally, CHAPTER 6 recapitulates the summary of the work.

CHAPTER 2. LITERATURE REVIEW

Since the current project revolves around computational calculation of FFR using CT angiography data, this chapter is going to build the necessary background required for this research. This chapter includes a collection of topics relevant to assessment of FFR computationally. Computational biomechanics is a multidisciplinary field including biology, medicine fluid mechanics and dynamics, mathematics, imaging and computer technology and modelling of coronary blood flows is of no exception.

This chapter is organised to present a group of topics related to discuss the applied methods in this thesis. The first section represents the physiology which focuses on the basic methods of coronary flow. Then basic fluid mechanics, computational fluid dynamics and governing equations are explained. Finally, the overlapping of the physiology of coronary arteries and fluid mechanics is explained, and mathematical modelling is developed.

2.1. Cardiovascular Disease

CVD involves heart and blood vessels and conditions affecting it. It includes the accumulation and development of fatty acids inside the arteries (atherosclerosis). The exact cause of CVD is unknown but there are lots of factors which may cause CVD i.e. High blood pressure, smoking, high cholesterol, diabetes, inactivity, obesity, family history, age, diet, alcohol etc.

There are four main types of CVD

1. **Coronary heart disease**

   This happens when the flow of oxygen-rich blood is blocked or reduced to the cardiac muscle which may cause angina (commonly known as chest pain), heart attack (suddenly blocked blood flow) and heart failure (heart suddenly stops pumping the blood flow)

2. **Stroke and Transient Ischemic Attack**

   Stroke is defined as the discontinued blood supply to a part of brain.

   A transient ischemic attack (TIA or “mini stroke”) is the disrupted blood supply to a part of brain temporarily

3. **Peripheral Artery Disease**

   When the blockage of blood is in the arteries which supply blood to the limbs

4. **Aortic Disease**

   It is the group of conditions affecting the aorta. The most common aortic disease is the aortic aneurysm in which aorta weakens and expands outwards which may cause it to burst and cause life-threatening bleeding.

2.2. Coronary Artery Disease

CAD also known as coronary heart disease (CHD) is a group of diseases which involves a reduced amount of blood flow to the heart muscles due to the accumulation of plaque in the arteries of the heart. It also includes sudden heart failure.

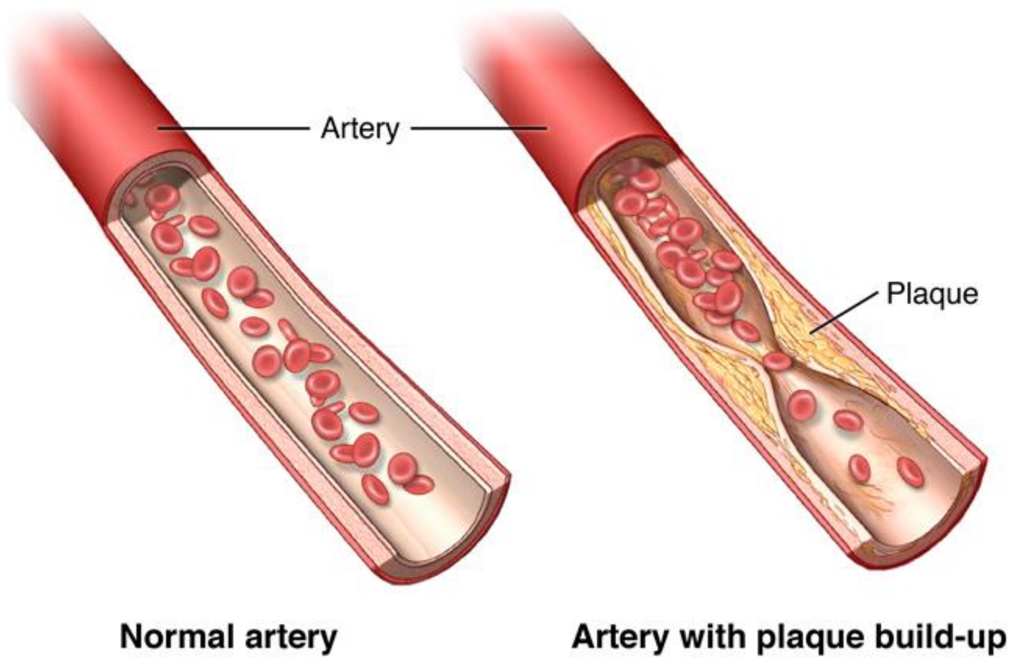

Figure 1: A Normal & Stenosed Artery [9]

These heart walls are composed of the myocardium which is most of the heart muscle tissue.

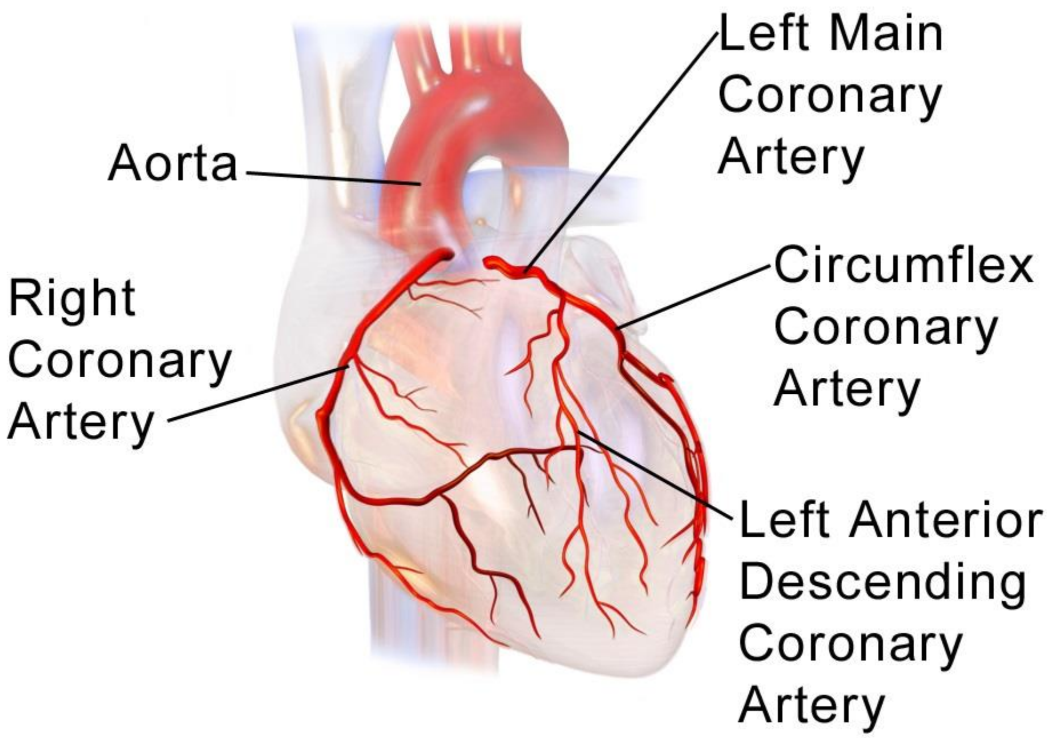

Figure 2: Anatomy of coronary arteries [10]

2.3. Left Anterior Descending Artery (LAD)

The left anterior descending artery is the one of the two main branches of left coronary artery. LCA takes oxygenated blood to anterolateral myocardium, apex and interventricular septum. It supplies major proportion of the blood to the left ventricle (LV) which is approximately 45-55% of the blood. Therefore, it is considered to be the most critical and life-threatening artery. Occlusion to this artery may cause widow maker infarction which may lead to death.

2.4. Computed Tomography Angiography (CTA)

In this technique, the vascular system inside the body is visualized i.e. vessels of the heart, aorta, lungs, kidneys etc. Images are created to search for blockages, dissections (tearing of walls), stenosis (narrowing in vessels) and aneurysms (dilations of the wall) by using a contrast agent (adenosine or papaverine) into the blood vessels.

2.5. Invasive Coronary Angiography (ICA)

ICA is the cornerstone of diagnosis and treatment of the patients with significant or unstable chest pain coronary artery disease (CAD). It is a medical imaging technique to visualize the lumen or blood vessels to detect any significant stenosis. It is traditionally done by injecting a contrast agent into the vessel which is administered by a catheter and imaging which is done by fluoroscopy.

2.6. Fractional Flow Reserve (FFR)

Fractional flow reserve is a novel and potentially clinically useful technique used to measure in coronary catheterization measure pressure differences across stenosis to determine the likelihood of a pressure drop which impedes oxygenated blood to reach heart muscles (a condition known as myocardial ischemia).

Fractional flow reserve is a patient-specific physiological index and it has been recognized as a gold-standard for the assessment of stable CAD [6, 7]. The prognosis of the functional severity of the stenosis in the coronary artery relies that how much the blood flow is obstructed.

During maximum blood flow, FFR is defined as the ratio of distal pressure to proximal pressure across a stenosis. It is given by

$$FFR = \frac{P_d}{P_p} \tag{1}$$

Where P_d is the pressure distal to the stenosis and P_p is the pressure proximal to the stenosis.

A value of FFR=0 means that the vessel is completely obstructed and a value of FFR=1 indicates a completely healthy artery. In clinical trial for DEFER studies, a cut-off point of 0.75 has been used [7].

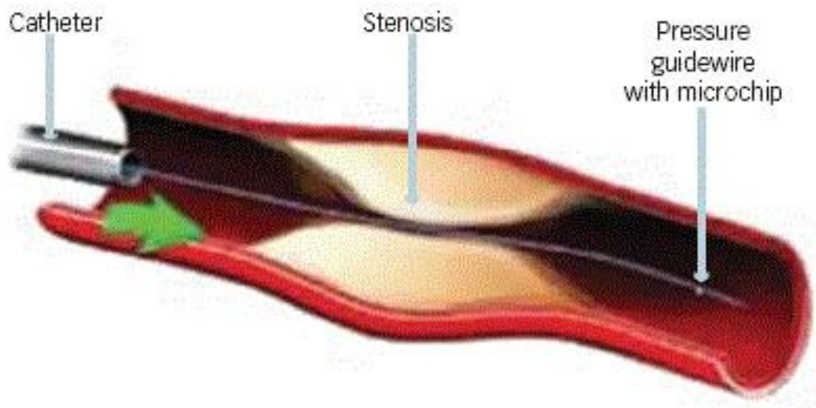

Figure 3: Measurement of Invasive FFR [11]

2.7. Computational Fractional Flow Reserve (FFR_{CT})

Computational fractional flow reserve is an emerging method to determine FFR by using calculations instead of measurements. Knowledge of various fields like computer science, artificial intelligence, medical imaging and computational fluid dynamics (CFD) are used for the simulation of the blood flow in the coronary artery to calculate the pressure drop across stenosis. By using these techniques from various dynamic fields, the clinical evaluation of FFR may evade the invasive procedure of coronary catheterization for the benefit of patients, doctors and health institutions, as it had been a headache for everyone. This is because these estimation procedures are inexpensive as compared to invasive FFR. Hlatky et al. has described that calculating FFR using CFD could decrease the costs by 30% while using to guide clinical examination procedures and 12% drop in post analysis of results [4]. These outcomes are also reinforced by numerous other researchers [3, 5].

While computing FFR_{CT}, CT DICOM images of a patient's heart are used to extract the 3D geometry of the coronary artery. This process of extracting coronary artery from the patient based DICOM CT scans is called segmentation. This 3D geometry is then induced to fluid dynamic equations and CFD results are obtained for pressure and velocity. To ensure the similarity with real blood flow, relevant patient-specific measurements are incorporated including some assumptions. Finally, the results are estimated at specific locations in the coronary arteries.

2.7.1. Previous work on FFR_{CT}

The diagnosis and in virtual assessment of individual treatments have already been proven valuable by applying the patient-specific mathematical models [8, 12]. Recent emerging imaging and computing technologies have contributed a lot to the highly refined and sophisticated computations in clinical procedures.

There are various research authorities around the world aiming to solve the encounters with *in-silico*[2] calculation of FFR. Amongst them, the most successful are HeartFlow, Inc. from Stanford University, who have received FDA[3] approval for their FFR_{CT} software to be used in clinical procedures as a commercial diagnostic tool. After raising $100M funding, they have also accomplished the level to be amongst the top 15 dealers in healthcare in 2016. However, FFR_{CT} methods must overcome a lot of encounters in terms of viability and accuracy. In the HeartFlow NXT trials [13], FFR_{CT} had sensitivity of 86%. Hence to increase the success of the clinical tools to overcome false negatives, it is need of the hour to increase the sensitivity.

In FAST FFR trials, FFR_{CT} (FFR_{angio}) has a sensitivity of 94% (95% CI, 88% to 97%) and specificity of 91% (86% to 95%). [14].

With a sensitivity of 80% Zhang et al. have assessed time-averaged flows. They have reported that working with pressure waveform, steady state marks a limitation [15]. But they have not discussed the importance of assuming steady flow for the estimation of FFR. With an accuracy of 88%, Tu et al. have achieved the simulation of 3D blood flows in 5 minutes. They have identified severe lesions, but they have not discussed whether and how the steadiness condition is contributing to FFR significantly. Morris et al. have achieved 97% accuracy by developing his methods and models in signifying severe stenosis in 35 patients from University of Sheffield [16]. Significant computational cost is required to simulate the pulsatile flows in developing coronary blood flows. Therefore, most research communities have agreed upon to develop stationary models over cardiac cycles to calculate FFR by using average flows and pressure.

Huo et al. have reported a slight importance to time averaged calculations of pressure drop across a stenosis focusing on the unsteadiness in *in vitro* experiments [17]. Mates et al. have

---

[2] *in silico*: From Latin, “performed on a computer or via a computer”
[3] FDA: Food and Drug Administration

reported the quasi-steady behaviour of stenotic coronary flows in similar experiments [18]. Although both steady and unsteady computations are well established in presented FFR_{CT} methodologies, none of the abovementioned studies explains their choice of insertion or omission of pulsatility in their models.

The Fractional Flow Reserve versus Angiography for Multivessel Evaluation (FAME) study evaluates the role of FFR in multivessel coronary artery disease [19].

A very limited studies can confirm that these results are also applicable to CFD simulations for $FFR_{CT.}$ The study by Bulant et al. [20] have published which reports the comparison of steady and transient simulations and evaluating slight nonconformities in FFR_{CT}. There is no research material available except these which have fully described the importance of the assumption of steadiness for the calculation of FFR in CFD simulations.

2.8. Coronary Blood Flow

Coronary arteries supply the myocardium with the oxygenated blood. The coronary arteries immediately branch off from the ascending aorta after the aortic valve. The coronary blood flow is the most distinguishing feature of the cardiovascular system as the blood flow is suppressed during systole [21]. Therefore, the coronary blood flow is found to be maximum during diastole, the relaxation phase of the cardiac cycle [22]. As the systolic pressure is considerably higher in the Left ventricle (LV) than in the right ventricle (RV), the pattern of maximal blood flow is more significant in LCA [23].

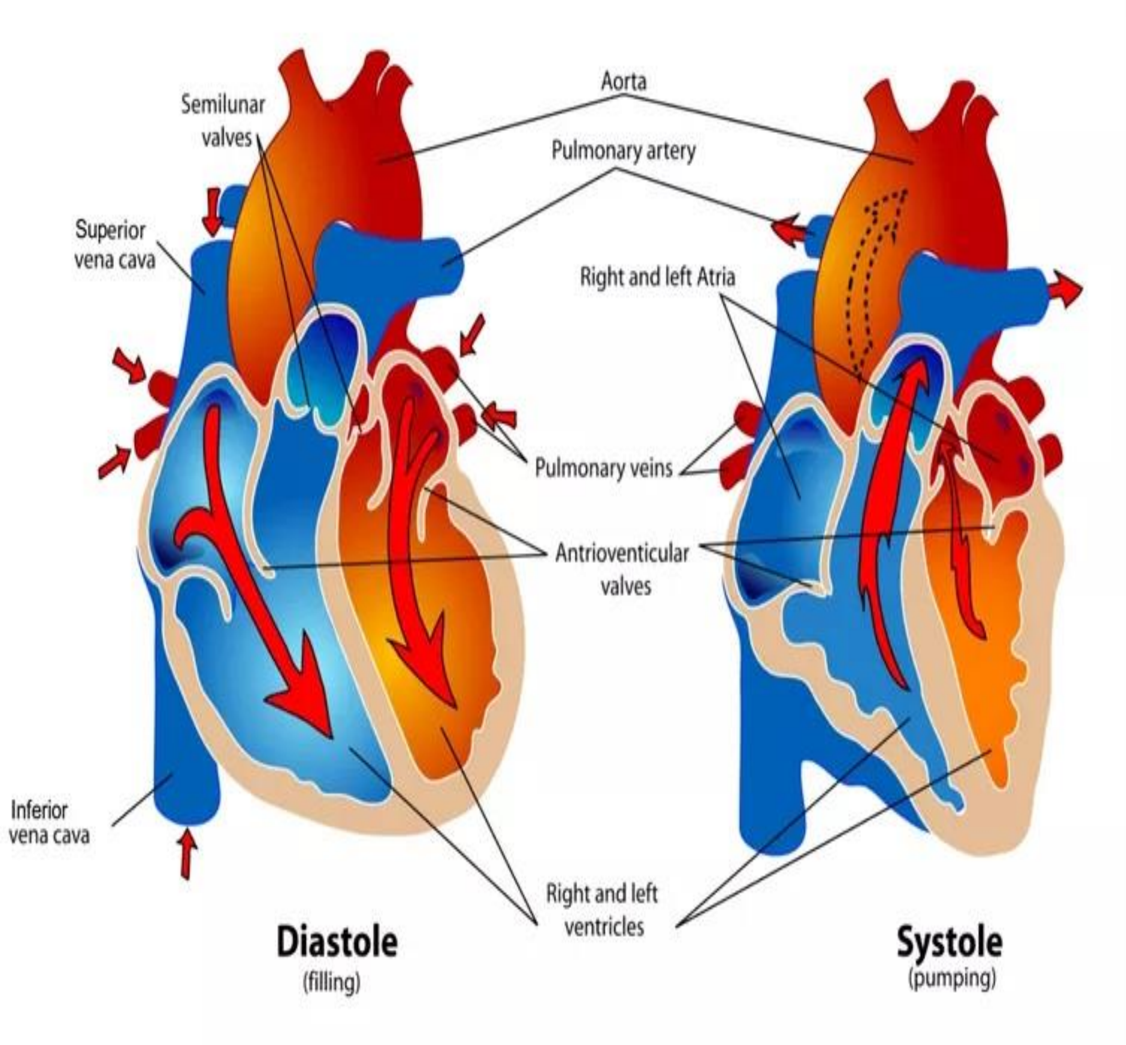

Figure 4: Blood Flow during Diastole & Systole [24]

2.8.1. Resistance to the Flow

Coronary flow is positive when the pressure in the proximal part of the coronary artery exceeds from the pressure in the distal part. In the human arterial system, the resistance to the blood flow is located in the arterioles in general [25] while under the normal circumstances, the contribution from the large coronary artery becomes negligible [22]. However, when a stenosis is present, then the contribution to the total resistance cannot be undermined rather than it is taken as significant. Young and Tsai have developed a formulae for the calculation of the pressure drop when narrowing is present [26], based on in vitro experiments

$$\Delta P_{stenosis} = \frac{K_v}{Re_D}\rho u^2 + \frac{K_t}{2}\left(\frac{A_0}{A_s} - 1\right)^2 \rho u^2 \tag{2}$$

where A_0 and A_s are the original and stenosed cross-sectional area respectively. For a given flow rate Q, eq becomes

$$\Delta P_{stenosis} = \frac{K_v \mu}{A_0 D_0} Q + \frac{K_t \rho}{2{A_0}^2}\left(\frac{A_0}{A_s} - 1\right)^2 Q^2 = a_1 Q + a_2 Q^2 \tag{3}$$

where D_0 is the lumen diameter without stenosis [25].

2.8.2. Baseline Conditions

On average, the resting or baseline coronary flow rate is approximately 225 ml/min [23]. The coronary blood flow distribution between RCA and LCA depends greatly upon the physiology of the coronary tree. The coronary arterial system may be right dominant of left dominant. Approximately 60% of the coronary blood flow runs through LCA in a right dominant coronary arterial tree; prevailing in 90% of the cases approximately. In the left dominant coronary tree, the blood flow in LCA is about 80% of the coronary flow [27].

2.8.3. Hyperaemia

Hyperaemia is the state of the maximal coronary flow. It works to the increased demand of oxygen by the myocardium. The arteriolar vasodilation, an auto-regulated expansion of the coronary arterioles, causes an increased blood flow by decreasing the peripheral resistance [28]. Hyperaemia can be triggered through exercise or by using the pharmacological agents.

Adenosine is a commonly used while measuring invasive FFR. It is difficult to estimate hyperaemic flow rates from the baseline conditions because of the varied individual response to the adenosine. In the response to the adenosine, hyperaemic flow rates are 2 to 5 times of the basal flow rates [29, 30]. Heart rate (HR) and aortic pressure are mildly affected by adenosine. In different studies a small to moderate increase in HR and an insignificant to small decrease in mean arterial blood pressure (MAP) has been observed [29, 31].

2.9. Fluid Mechanics

The exquisite behaviour of the fluids never seems to temper the human curiosity in the perpetual search for the understanding of the nature.

2.9.1. Governing Equations

The Navier[4]-Stokes[5] (N-S) equation is Newton's 2nd law expressed for fluids in Eulerian approach which describes a balance of fluid forces with the rate of change of momentum.[32]. To completely describe the fluid motion, we also need to explain the conservation of mass that's why, in CFD terminology, fluid equations are referred to both the continuity equation and momentum equation (N-S equation). The conservative form of the fluid equations are [33]:

$$\frac{\partial \rho}{\partial t} + \nabla.(\rho U) = 0 \tag{4}$$

$$\frac{\partial (\rho U)}{\partial t} + \nabla.(\rho U \times U) = -\nabla p + \nabla.\tau \tag{5}$$

$$\tau = \mu\left(\nabla U + (\nabla U)^T - \frac{2}{3}\delta\nabla.U\right) \tag{6}$$

Equation 4 is the continuity equation which expresses the conservation of mass and equation 5 is the vector equation which contains three momentum equations. P is the pressure, u is the velocity, t is the time, ρ is the density and μ is the viscosity. ρ and μ are material constants.

The left-hand side of the momentum equation shows the transient and spatial acceleration of the fluid. On the right-hand side of the momentum equation, the first term explains the pressure forces and the second term expresses the viscous forces.

Solving N-S equations requires simplification of assumptions using numerical methods for applied problems. The analytical solutions are only obtainable for very simple differential equations with simple boundary conditions (BCs) and geometrical configurations.

---

[4] Claude-Louis Navier (1785-1836): French Mechanical Engineer & Physicist
[5] Sir George Gabriel Stokes (1819-1903), 1st Baronet: an Anglo-Irish Physicist and Mathematician

Assuming rigid walls, in a pipe of constant circular cross-sections, steady and laminar flow, an analytical solution to the N-S equations for simple flows can be given by Poiseuille[6] equation. The velocity profile for the Poiseuille equation is given as

$$\Delta p = \frac{8\mu L Q}{\pi R^4} \tag{7}$$

The Poiseuille equation shows that the velocity profile is parabolic. Integrating the equation over the cross section gives the volumetric flow rate as

$$Q = \frac{\pi r_1^4}{4\mu} \frac{dP}{dx} \tag{8}$$

For the conditions where the assumption of rigid, variable circular cross-sectional cylinders can't be justified, equations become inadequate. In such cases the exact solution cannot be obtained analytically, and N-S equations are solved using numerical methods. This field of study is called computational fluid dynamics (CFD).

2.9.2. Computational Fluid Dynamics

Sufficient research has already been done for the validation of numerical solution algorithms and it has been ensured that the establishment of CFD can be used as an essential tool in the paradigm of modern fluid mechanics. Nevertheless, it cannot be ensured whether smooth solutions to the N-S equations always exist.

2.9.3. Finite Element Method

In FEM, the N dimensional spatial domain (control volume (CV)) containing the physical system is partitioned into a finite number of cells. These cells are called elements where to determine the order of the element, each element is facilitated with interpolation function i.e. linear, quadratic.

---

[6] Jean Léonard Marie Poiseuille (1797-1869): A French Physicist & Physiologist

For the governing differential equations, in the weak form representation, an arbitrary weighting function w is multiplied with the variables of the governing differential equation before integrating over the domain to reduce the degrees of the derivatives [34].

The N-S equation on weak form is shown in the equation.

$$\int_{\Omega} w.\frac{\partial u}{\partial t} d\Omega + \int_{\Omega} w.(u.\nabla)u d\Omega + \int_{\Omega} \frac{P}{\rho}\nabla.w d\Omega + \int_{\Omega} \nabla w : \nu\nabla u d\Omega = 0 \tag{9}$$

2.9.4. Newtonian and non-Newtonian Fluids

A Newtonian fluid is that in which viscosity remains constant with increasing or decreasing shear rate. It is given by

$$\tau = \mu\frac{\partial u}{\partial y} = \mu\dot{\gamma} \tag{10}$$

A non-Newtonian fluid viscosity does not remain constant with increasing or decreasing shear rate. Hence a non-Newtonian fluid is of two types.

1. **Shear Thinning**

   These types of fluids exhibit a decrease in viscosity with increasing shear rate e.g. toothpaste, bottle of ketchup.

2. **Shear Thickening**

   These types of fluids follow an increase in viscosity with increasing shear rate. The best example for a shear thickening fluid is a mixture of corn-starch with water.

There are various non-Newtonian models available to explain the viscous behaviour of fluids. These are

1. Carreau Model
2. Power Law Model
3. Bingham-Papanastasiou Model
4. Herchel-Bulkley-Papanastasiou Model
5. Casson-Papanastasiou Model

Carreau Model:

The Carreau Model is based on Power Law Model which explains the behaviour of non_Newtonian fluids on the basis of shear rates [35]. This is,

$$\mu = \mu inf + (\mu 0 - \mu inf)[1 + (\lambda\dot{\gamma})^2]^{\frac{n-1}{2}} \tag{11}$$

$$\dot{\gamma} = \max\left(\sqrt{2S{:}S},\ \dot{\gamma}_{min}\right) \tag{12}$$

$$S = \frac{1}{2}[\nabla u + (\nabla u^T)] \tag{13}$$

Table 1: non-Newtonian properties of Blood

Parameter	Variable	Value	Unit
Zero shear rate viscosity	μ_0	0.056	Pa.s
Infinite shear rate viscosity	μ_{inf}	0.0035	Pa.s
Model Parameter	λ	3.313	s
Model Parameter	n	0.3568	1

2.9.5. Computational Fluid Dynamics (CFD) Methodology

Implementation of CFD methodology involves programming of the solution algorithms. Various open-source and commercial softwares are available which come with built in programs and algorithms. Irrespective of the choice, the methodology of the CFD remains same which involves few steps.

1. Meshing

Meshing is the process of subdividing the computational domain into elements, nodes or control volumes depending upon the method opted for the solution. Based of mathematical principles, certain algorithms are also used in softwares for generating the meshes of high quality.

2. Pre-processing

In this process, fluid mechanical properties are defined for the fluid flow problem. Physics of the simulation is first defined such as fluid flow, turbulence modelling, thermal conductivity, etc. Then the study is defined i.e. steady or transient etc. Material properties for blood are dispensed to flow volume of the domain e.g. density, viscosity etc. Finally, boundary conditions (BCs) are imposed.

3. Solution

Solution algorithms are chosen to solve the fluid flow problem such as FEM, FDM, FVM etc. The convergence criterion is also defined i.e. time steps, number of iterations etc. Certain numerical parameters are also defined which control the solution process such as relaxation factors, numerical diffusion coefficients, conductance, compliance etc.

4. Post-processing

The final step is the post processing. Certain type of 1D, 2D and 3D plots are used to aid the visual inspection of the obtained results for field variables of different parameters such as velocity and pressure etc.

2.9.6. Errors in CFD

CFD is based on numerical methods which are estimations and approximations, hence they are also associated with errors. In CFD, the errors are described as:

1. Modelling Errors

The modelling errors occur from the inconsistencies between numerical and actual physical systems. The errors are associated with simplification of PDEs and BCs and not from numerical approximations. That's why validation of the obtained simulation results is important to evaluate and minimize modelling errors.

2. Discretization Errors

These errors are also called truncation errors because they arise from discretization of partial differential equations. [36].

3. Convergence Errors

These are associated with the iterations. Consecutive iterations explain the variation in the solution. This represents the quality of convergence. Iterative errors occur both in time and solution algorithms.

4. Round-off Errors

These errors occur because in each floating-point number, only a certain number of digits can be stored.

The errors in CFD can be measured through verification and evaluation of the magnitude of improvement for the solution. In the assessment of CFD results, verification and validation play major roles. Validation ensures that a mathematical model exactly represents the physical problem to be discussed and its characteristics. Validation is the ensuring that the mathematical equations are correctly solved caused by implementation and discretization by examining the errors.

2.9.7. Boundary Conditions

The boundary conditions are specified in any computational model. Boundary conditions are expressed as the value of a field variable (Dirichlet BCs) or the value of its gradient (Neumann BCs).

When performing a CFD simulation, velocity or pressure is specified on the boundaries (inlets and outlets). For rigid walls, inlet and wall conditions can be employed readily, while outlet conditions are most significant for the final results for FFR and subjected to great uncertainties [37, 38].

In our computational model of coronary arteries, CT Angiography images are used and refined to get the image data of sufficient quality to obtain a 3D domain. This 3D domain is then curtailed for those features which are unable to be captured by CT.

1. Walls

Walls are either rigid or compliant. Usually the no-slip boundary condition is applied on the wall of the artery which means that velocity is zero on the wall. For a non-solid wall, a fluid-structure interaction mechanical problem is solved which cause more computational expense. Hence it is more recommended to assume rigid walls to avoid computational complexity, unless it does not significantly affect the functional similarity of the simulation model.

2. Inlets

Clinical measurements are well estimated at the inlet of a coronary artery. Arterial blood pressure can be measured to obtain aortic pressure waveforms. Flow rates can be measured non-invasively using Transthoracic Doppler Echocardiography (TTDE) in the main coronary branches [39].

3. Outlets

If a flow rate or a pressure is imposed at outlet, then it would compel the solution to match. Another approach possible to meet the resistance in the branches to let the flow distribute in the 3D domain which are offered to the blood flood. In this way, at the outlet, the total peripheral resistance is endured [22]. For that purpose, the Windkessel Model is used widely but the problem with this approach is that it is further based on many assumptions to calculate resistance, inductances and compliances. That is why it is better to use an outlet pressure to match the diastolic pressure to simplify the computational model. Other methods to determine peripheral resistances are based on empirical observations.

2.10. Pulsatile flow

Pulsatile flow is a transient flow problem in which a periodic, time-dependent pressure gradient is imposed to produce a time-dependent motion. It is given by [35],

$$-\frac{\partial P}{\partial z} = G = G_0(1 + \epsilon \sin \omega t) \tag{14}$$

In a real problem of a pulsatile flow like in an artery, the walls are compliant and the cross-section is not circular. In pulsatile blood flow and other applications, we are only concerned with the solution which has been obtained after sufficiently long time after imposing the pulsatile pressure gradient to make sure that the velocity field is strictly periodic. Hence, we don't much care whether the pulsatile flow starts from rest. A more complicated periodic pressure gradient and velocity profile can be achieved using Fourier Transform. The complex $G(t)$ is decomposed into discrete set of sinusoids.

The governing differential equation for velocity profile can be given as

$$\rho \frac{\partial u_z}{\partial t} = G_0(1 + \epsilon \sin \omega t) + \mu \left[\frac{1}{r}\frac{\partial}{\partial x}\left(r \frac{\partial u_z}{\partial r}\right)\right] \tag{15}$$

CHAPTER 3. METHODS

This chapter details the methodology involved in developing and applying CFD simulation for the calculation of FFR non-invasively in LAD. The first section describes how the computational models are employed for the coronary flow simulations. Section 3.1 describes how the numerical methodology was developed and the patient data and patient specific simulations are described in section 3.2. Section 3.3 describes the numerical methods employed. The methodology has been developed gradually and by continuous verification and validation.

3.1. Computational Model

The computational model employed in this work is composed of CFD simulations applied on a 3D volume of LAD to solve N-S equations. Input to the computational model is a pulsatile and non-pulsatile velocity at the inlet and a constant outlet pressure. No-slip boundary condition is applied at the wall. The geometric model of LAD is shown in Figure 5.

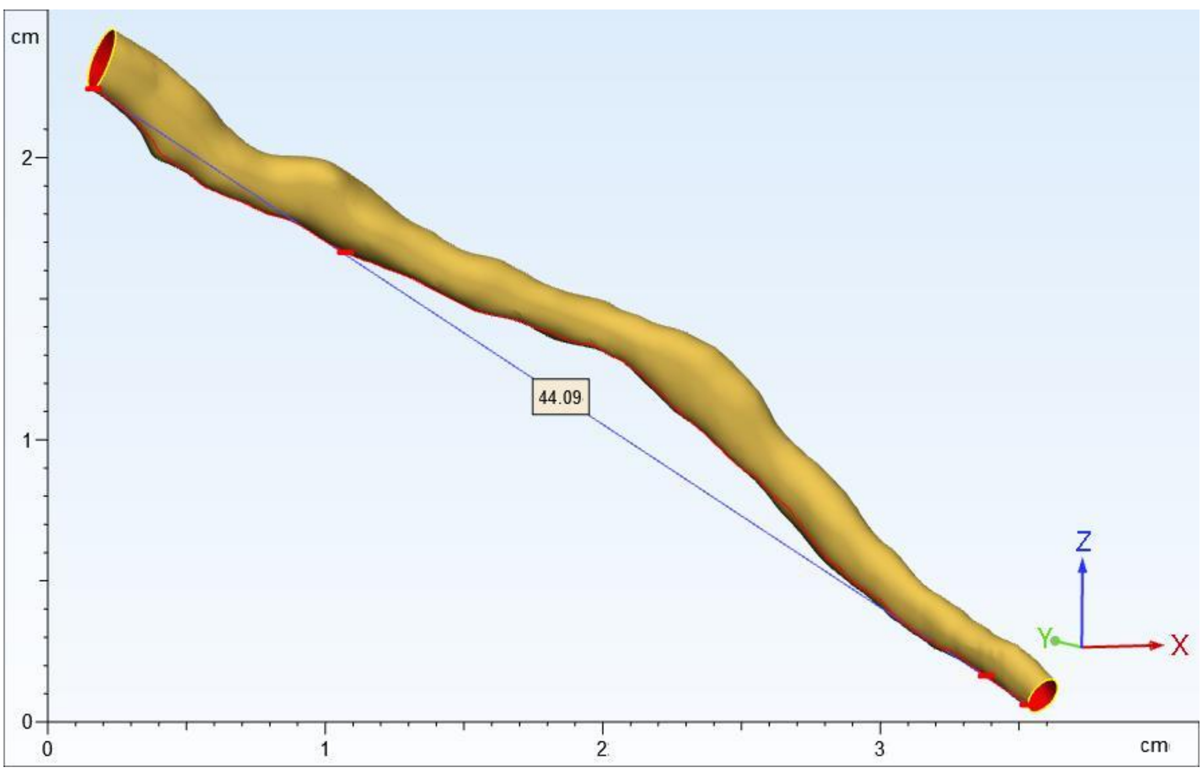

Figure 5: Geometric Model of Left Anterior Descending

The softwares used in the present work are

1. **Mimics materialize**

Mimics is a medical imaging processing software which is used to create 3D geometries from 2D image data of CT and MRI. It comes with two packages i.e. Mimics and 3-Matic. Mimics models the 3D geometry from DICOM images while 3-Matic is used for segmentation and to generate meshes.

2. **COMSOL Multiphysics**

COMSOL Multiphysics is a finite element-based Multiphysics solver. It allows modelling and simulation of conventional physics-based user interfaces and couple system of partial differential equations.

3.2. Patient-Specific Model

Angio-CT scans were acquired from AFIC (Armed Forces Institute of Cardiology) on patient consent and were implemented on this study. Computed Tomography Angiography (CTA) images are obtained from a patient who was willing to contribute in the research project to develop patient-specific model.

3.2.1. Physiological Parameters

There are some parameters which were obtained from the literature. This includes the rheological properties of blood ρ=1060 g/cm3. The blood had been assumed as non-Newtonian. The patients-specific parameters employed are Patient's blood pressure i.e. diastolic and systolic blood pressure has been obtained and ECG was measured. Heart rate of the patient was 72 bpm.

3.2.2. Patient-Specific Data

The patient had volunteered for the research project and his privacy was kept confidential. The patient-specific data is

Table 2: Patient-Specific Data

Age	**Sex**	**Hospital**	**Heart Rate**	**SBP**	**DBP**	**FFR_{inv} with Adenosine**
55	Male	AFIC	72	130	80	0.99

3.2.3. Pulse Sensor Data

Pulse sensor is simple heart sensor which is used to monitor pulsatile flow nature in arteries. It is used as a plug-and-play sensor with Arduino. A pulse sensor has three wires.

- Black pin as a ground wire
- Red wire showed Vcc supply voltage
- Pink wire as a pulsating signal wire

The ground wire has been connected to the ground (GND) pin of Arduino mega. Vcc supply voltage connected with 5V input pin of Arduino mega. Signal pin has been associated to the A0 analog input pin of the system. It is usually placed on index finger. It generates pulses of heartbeat PQRS. The data accurately captured and displayed the pulse waveform is shown in the figure

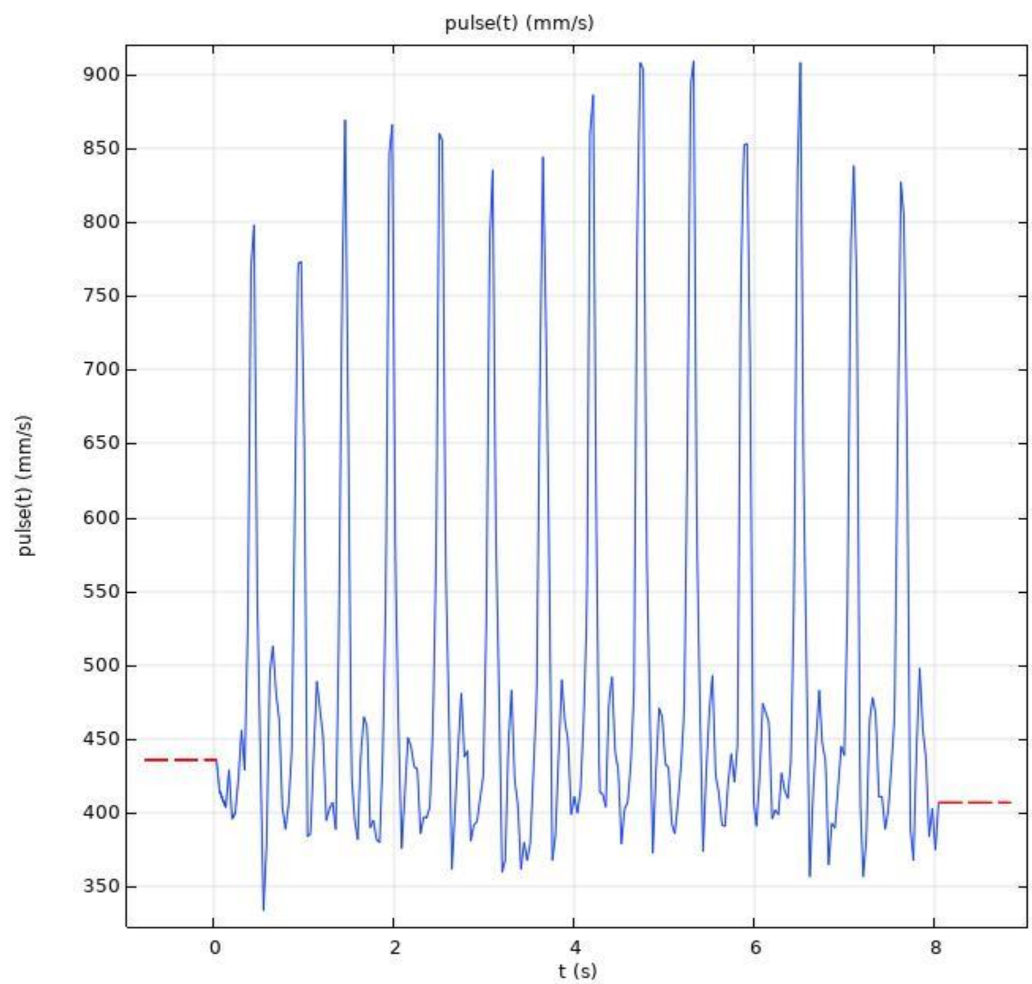

Figure 6: PQRS obtained using pulse sensor

3.2.4. Segmentation

CTA images of the patient were imported into an advanced image processing suite (Here Mimics Materialize) and a geometry was created for LCA using Hounsfield Units (HU)>=226. This LCA was then exported to 3-matics software and LAD was segmented. Segmented geometry was then exported as *.stl* file which was further used as an input model in COMSOL Multiphysics platform.

The pipeline for modelling and segmenting LAD is:

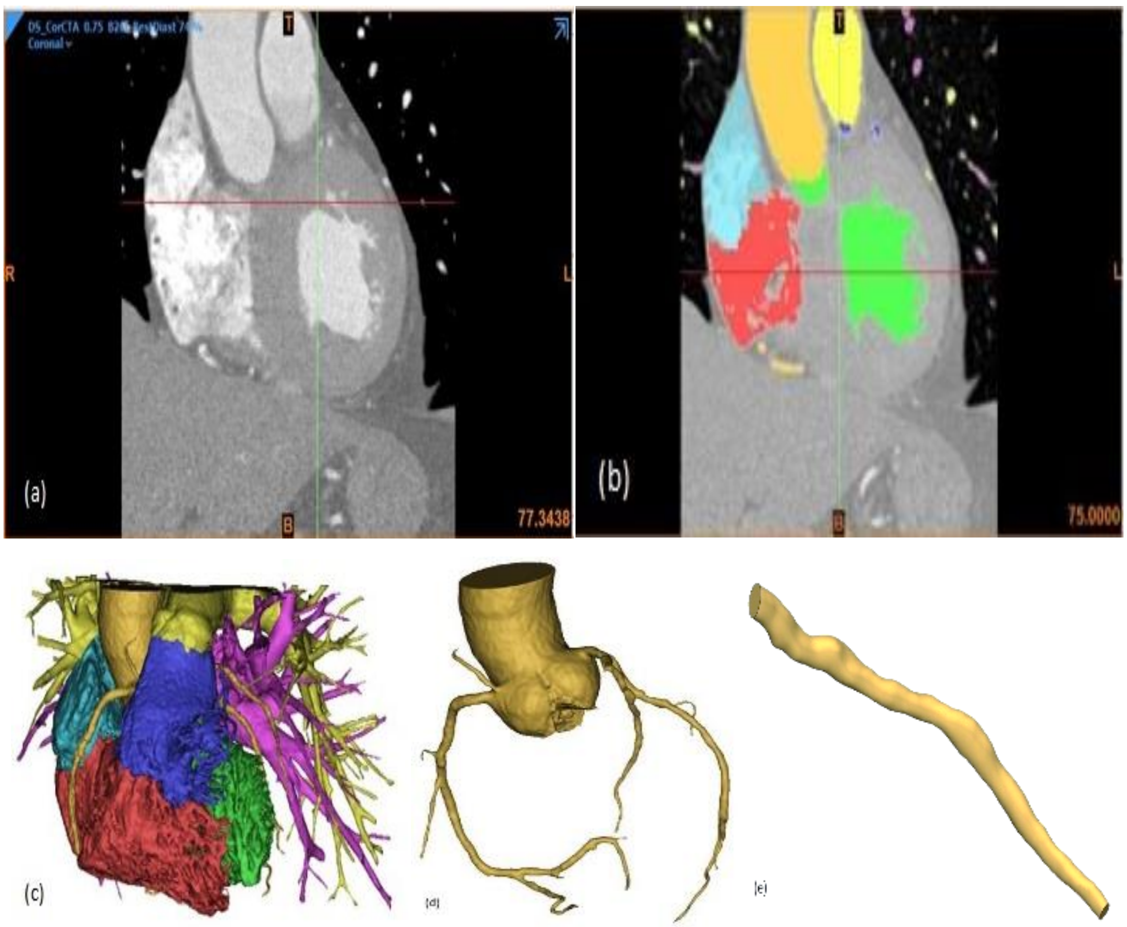

Figure 7: Workflow for segmenting LAD in Mimics Materialise

3.3. Numerical Methods

3.3.1. Computational Fluid Dynamics

The computational model is governed by fluid flow equations with velocity is applied at inlet and pressure is specified at the outlet. Linear Lagrange P1 tetrahedral elements are applied for interpolation for velocity and pressure field variables. In stationary case, the simulations were run for 1000 iterations. In transient simulation, time step ΔT is 0.001s and simulations are run for 800 cycles with a period of 0.8 s for non-pulsatile flows. For pulsatile flows, a single pulse is simulated with a single pulse of time period of 0.8 s and the time step is chosen to be 0.001 s to run the simulation for 800 cycles.

The laminar flow from fluid flow physics module has been used to simulate blood flow This provides high performance implementation of the schemes to solve fluid flow problems for continuity and momentum equations. The PARDISO Solver is used to solve the coupling of velocity and pressure fields. PARDISO is a robust and memory efficient tool for solving the asymmetric linear systems of equations as compared to Mumps and Spool.

3.3.2. Boundary conditions

BCs are assigned to inlet, outlet and wall of the geometry obtained from 3-Matic software. The wall of the CA is assumed as solid with no-slip boundary condition for all simulations.

3.3.2.1. Steady Boundary Conditions for non-Pulsatile Flow

For steady simulations, a constant velocity of 0.30 m/s is given at the inlet and a constant outlet pressure of 80 mmHg is assumed at the outlet to mimic the patient specific parameters.

3.3.2.2. Transient Boundary Conditions for non-Pulsatile Flow

For non-pulsatile flow, BCs were applied same as the steady state and a time period of 0.8 s is used with a time step of 0.001 s.

3.3.2.3. Transient Boundary Conditions for Pulsatile Flow

For pulsatile flow, a single pulse of 0.8 s is also coupled with the steady BCs. A single pulse employed to develop pulsatile flow is shown in

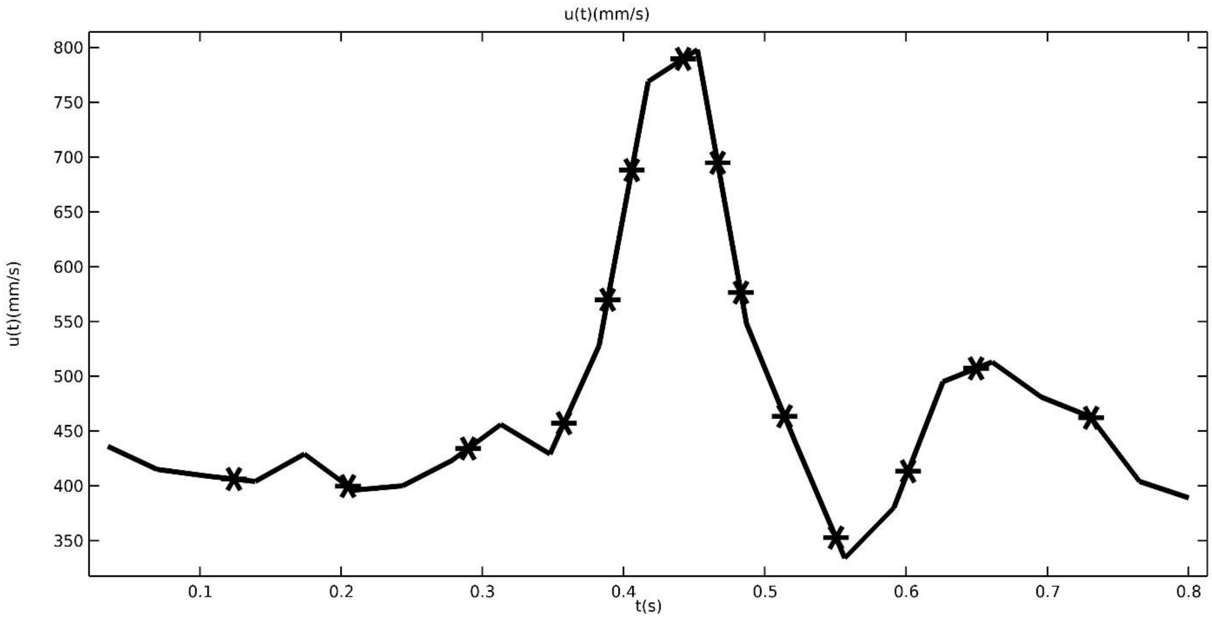

Figure 8: Velocity Profile of the Pulsatile Flow

3.3.3. Pre-processing

The LAD model was imported in COMSOL Multiphysics and boundaries (inlet, outlet and wall) are defined. Fluid flow physics was defined. Stationary and transient simulations were studied for a non-Pulsatile flow. Transient simulations were studied for pulsatile flow. The properties of blood (density and non-Newtonian Carreau Model viscosity) are assigned to the 3D domain. Further incompressible fluid flow equations and BCs are assigned.

Meshing

Meshing is the most important part of a computational problem. COMSOL Multiphysics is an FEM based solver. In the presented methodology, the P1 tetrahedral mesh is selected. The properties of mesh are:

Table 3: Properties of Mesh

Maximum Element Size	0.771 mm
Minimum Element Size	0.0833 mm
Maximum Element Growth Rate	1.1
Curvature Factor	0.4
Resolution of Narrow Regions	0.9

The total number of elements generated are approximately 0.1 M including 92911 domain elements, 8376 boundary elements and 86 edge elements.

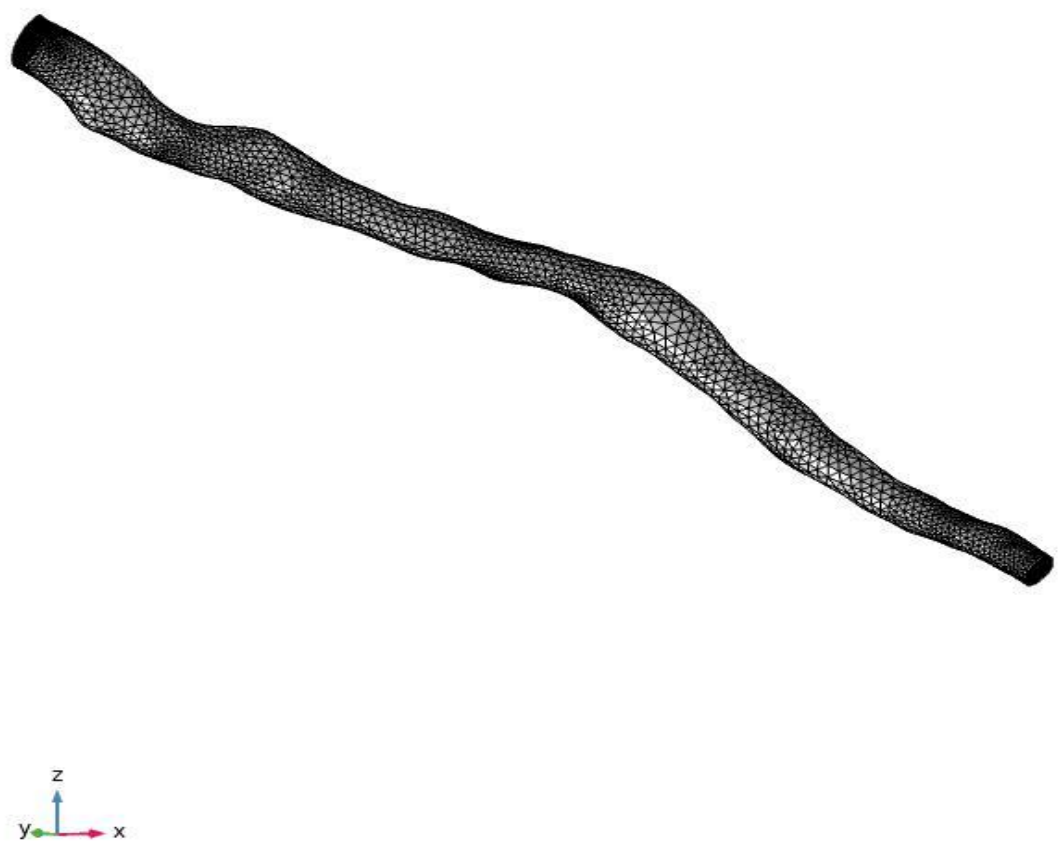

Figure 9: Mesh of LAD

3.3.4. Processing

Stationary and Transient simulations for non-pulsatile flow and transient simulations for a pulsatile flow are studied. The configurations for these studies are:

3.3.4.1. Stationary Study for non-pulsatile flow

Non-linear Newton Method is opted for the Algebraic Multigrid Solver configuration. The initial damping factor was 0.01 while minimum damping factor is 10^{-6}. Direct PARDISO solver was used and the solution is run for 1000 iterations. The convergence criterion is set to 10^{-3}.

3.3.4.2. Transient Study for non-pulsatile flow

The similar configurations are used for transient simulations as used for stationary steady. The time period for transient simulation is 0.8 s and the time step is 0.001 s. Hence the simulation was done for 800 iterations.

3.3.4.3. Transient Study for pulsatile flow

The similar configurations are used for pulsatile simulations as used for stationary non-pulsatile simulations. The time period which depends upon the patient's heartbeat was chosen as 0.8 s and the time step is 0.001 s. Hence the simulation is done for 800 iterations. In a pulsatile flow, a pulsating function of velocity profile is coupled with the inlet velocity.

3.3.5. Post processing

The results are obtained for velocity and pressure which are presented in RESULTS chapter.

CHAPTER 4. RESULTS

In this chapter, all the results are presented which were obtained from different simulation studies. Section 1 presents all the results and section 2 compares all the results with invasive FFR.

4.1. Computational Results

This section presents all the results which were obtained in COMSOL Multiphysics for different simulations.

4.1.1. Stationary Study for non-pulsatile flow

The BCs and stationary model was setup as explained in section 3.3.2.1 and 3.3.4.1. The simulation results for velocity and pressure are

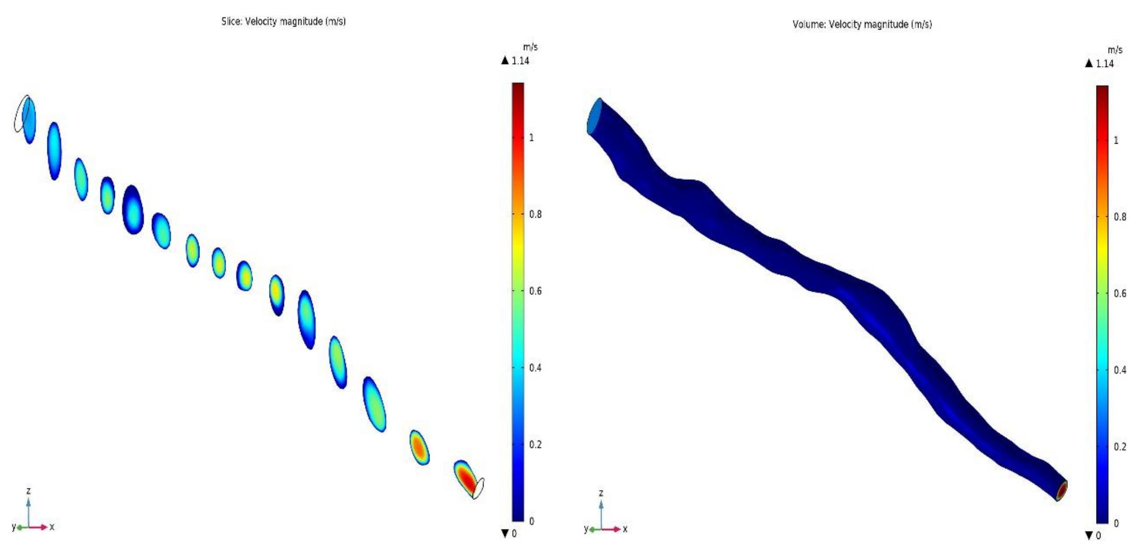

Figure 10: Simulation Results for Velocity (Slice & Volume plots); Stationary Study for non-Pulsatile Flow

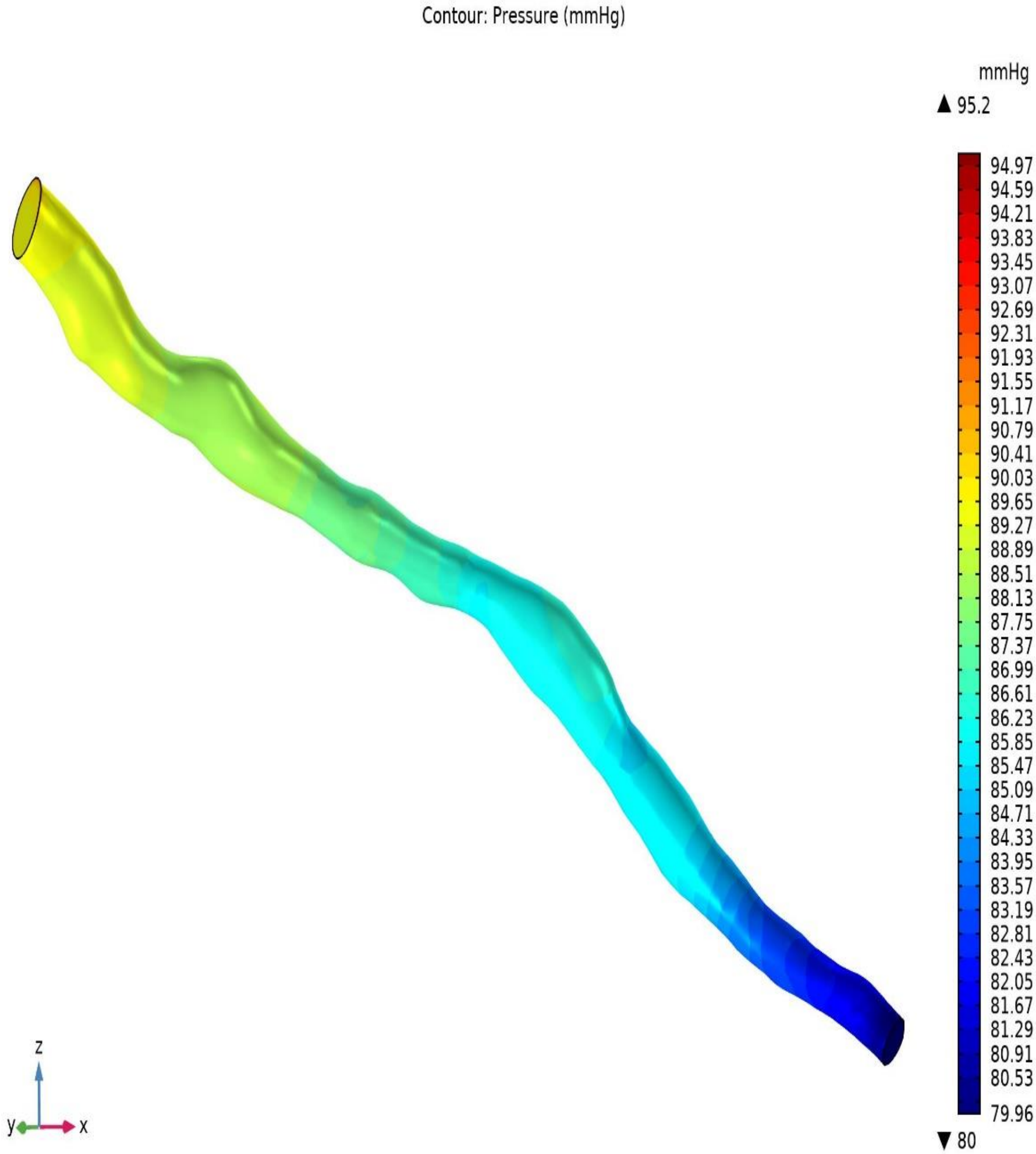

Figure 11: Simulation Results for Pressure; Stationary Study for non-pulsatile flow

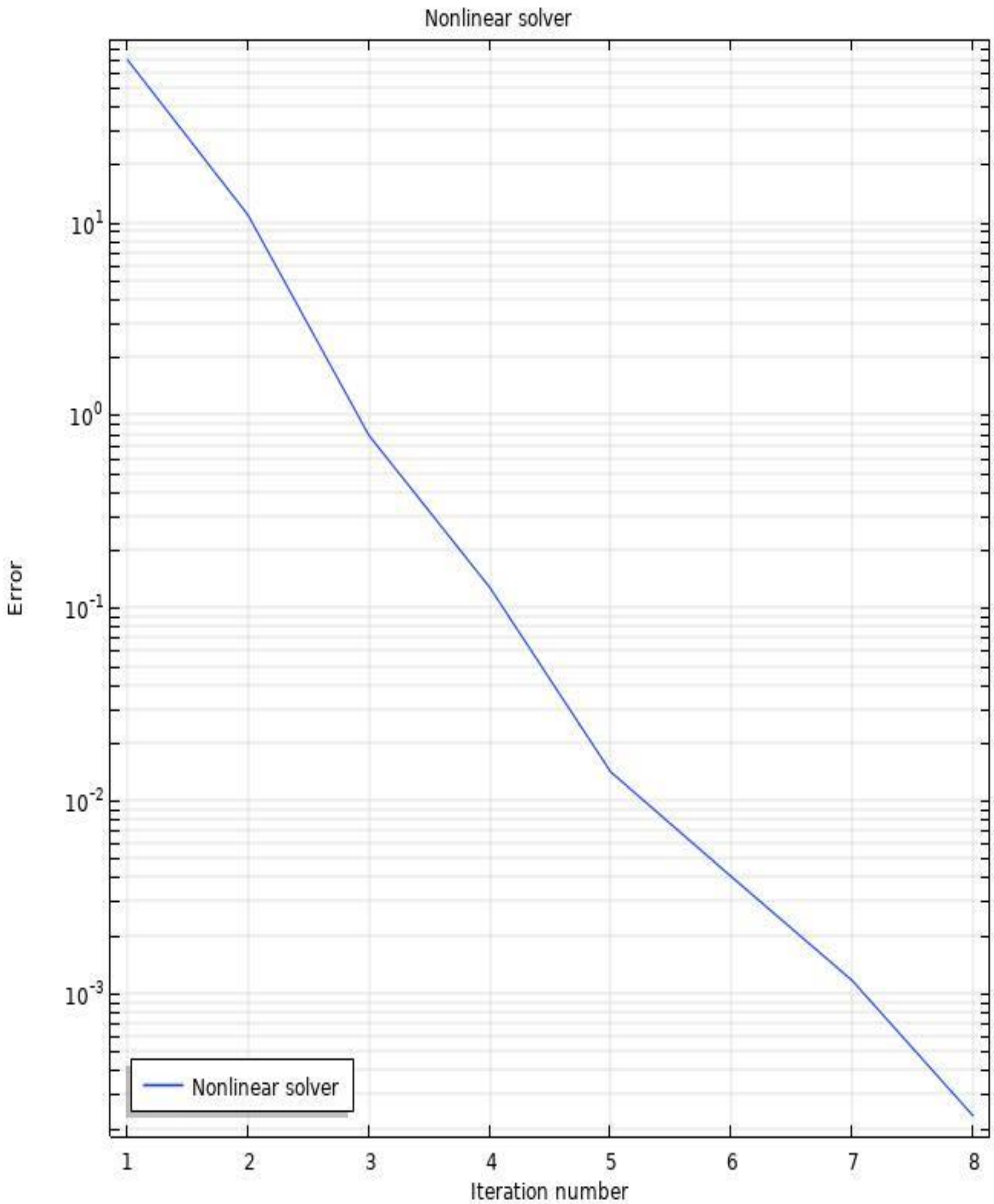

Figure 12: Simulation Results for Convergence; Stationary Study for non-Pulsatile Flow

4.1.1.1. Transient Study for non-pulsatile flow

The BCs and stationary model was setup as explained in section 3.3.2.2 and 3.3.4.2. The simulation results for velocity and pressure were obtained. The convergence for the simulation is shown in figure.

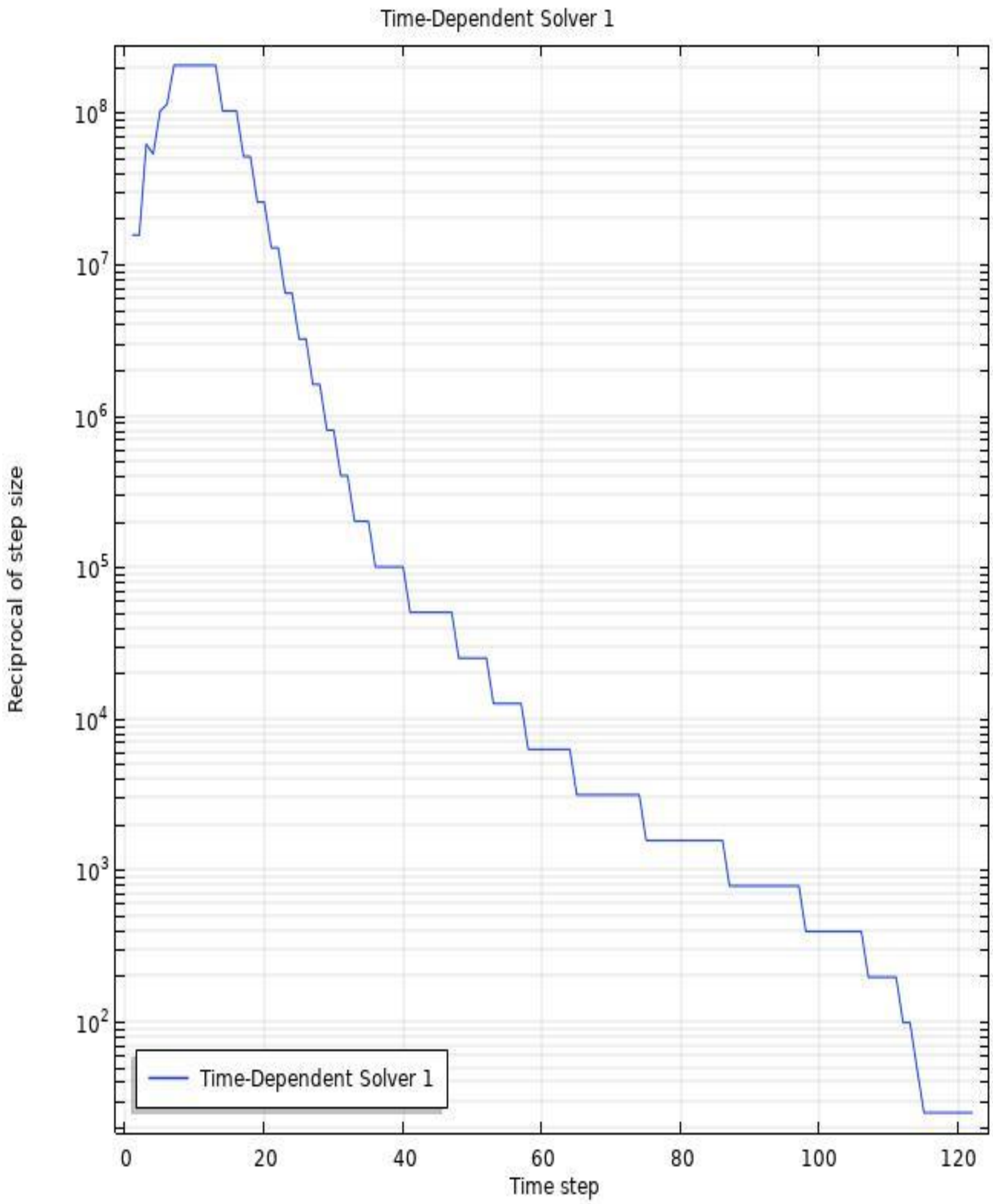

Figure 13: Simulation Results for Convergence; Transient Study for non-Pulsatile Flow

4.1.1.2. Transient Study for Pulsatile flow

The BCs and stationary model was setup as explained in section 3.3.2.3 and 3.3.4.3. The simulation results for velocity and pressure were obtained. The convergence for the simulation is shown in figure.

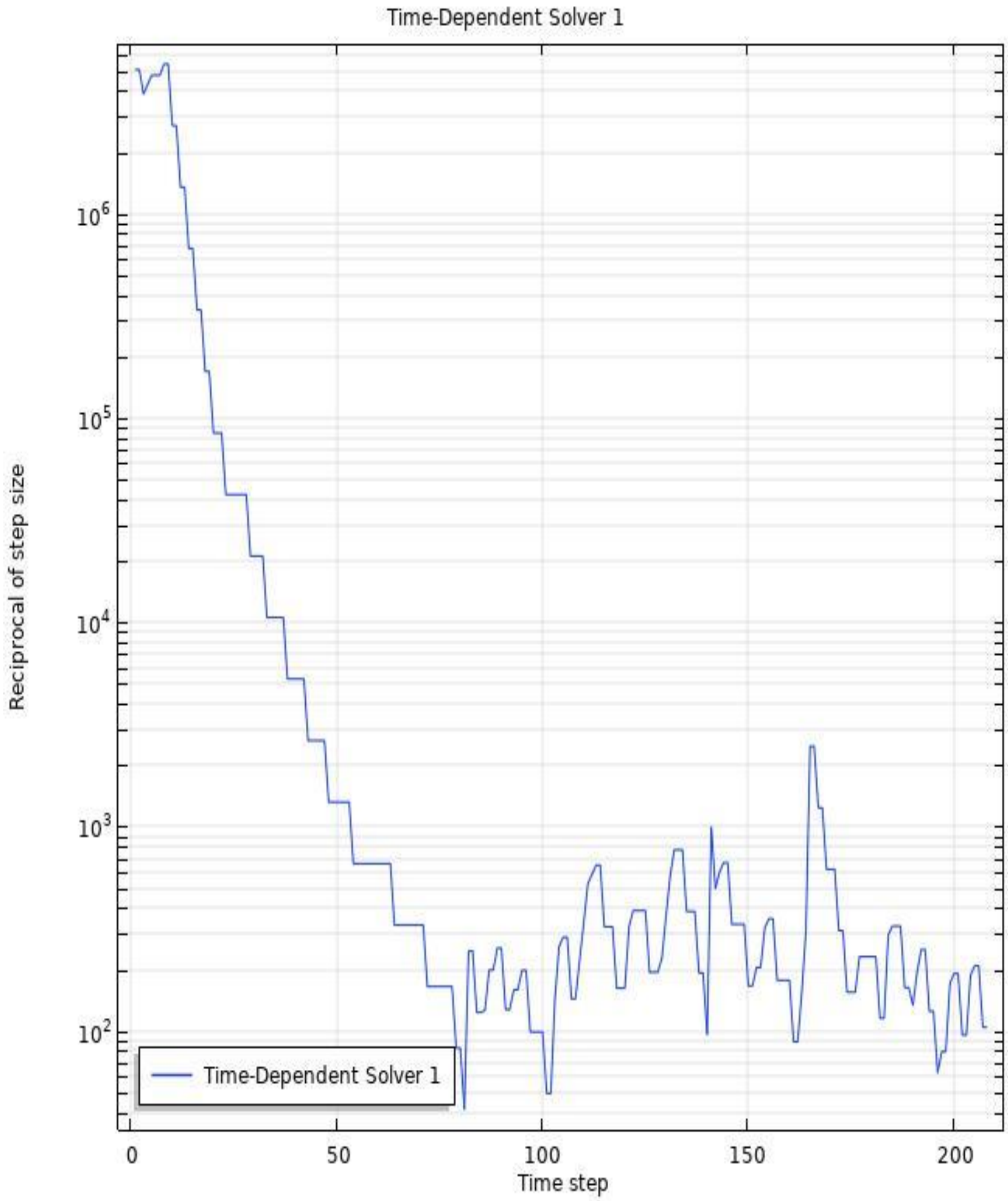

Figure 14: Simulation Results for Convergence; Transient Study for Pulsatile Flow

4.2. Comparison of non-Pulsatile and Pulsatile Flows

No significant stenosis was observed in CTA DICOM images, but a narrowing was found in the middle of LAD as shown in the figure.

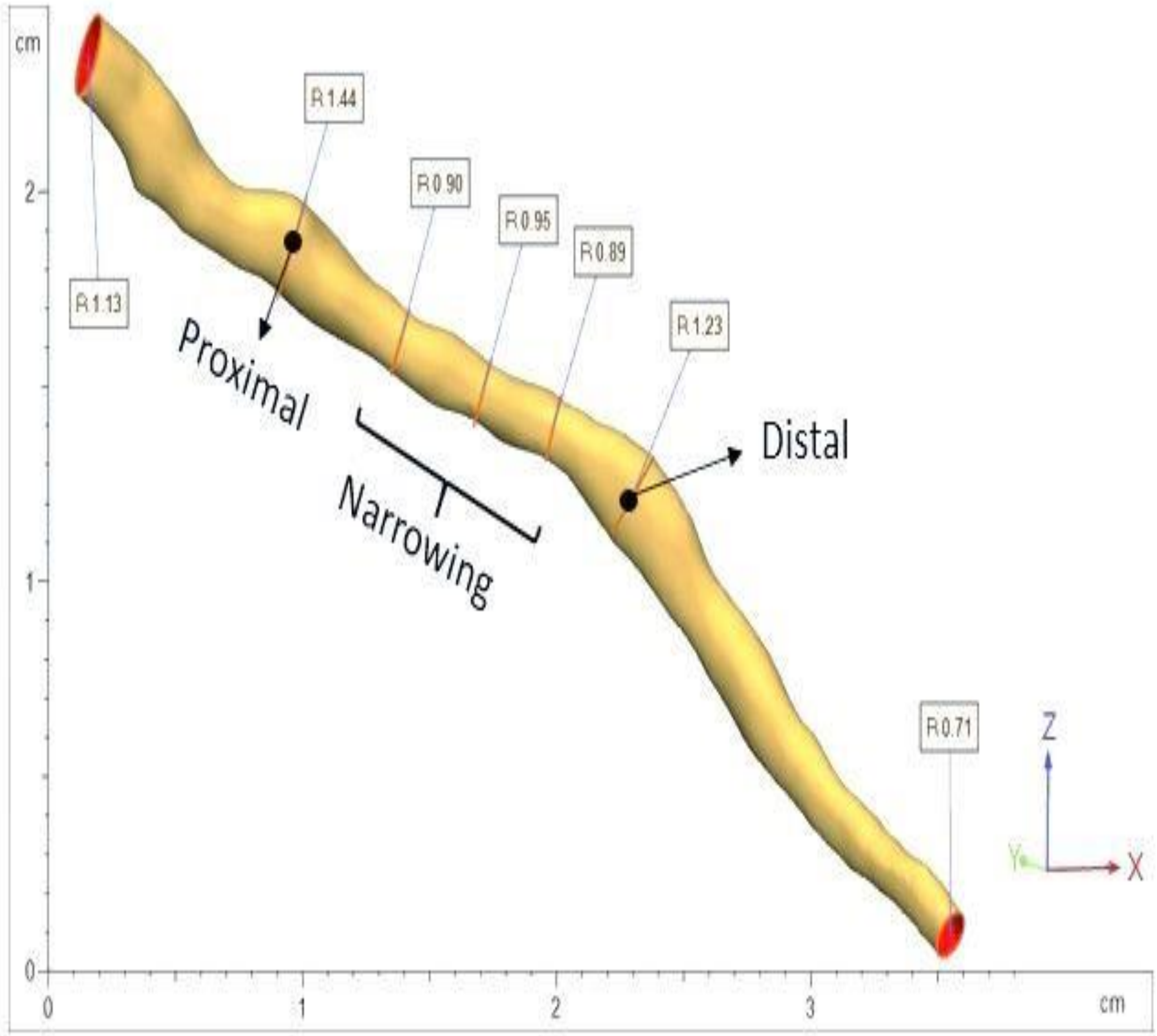

Figure 15: Proximal and Distal locations across the narrowing (all measurements are in mm)

Pressure was calculated proximal and distal to the narrowing. FFR was obtained using eq.1 at each time step for both pulsatile and non-pulsatile transient blood flows.

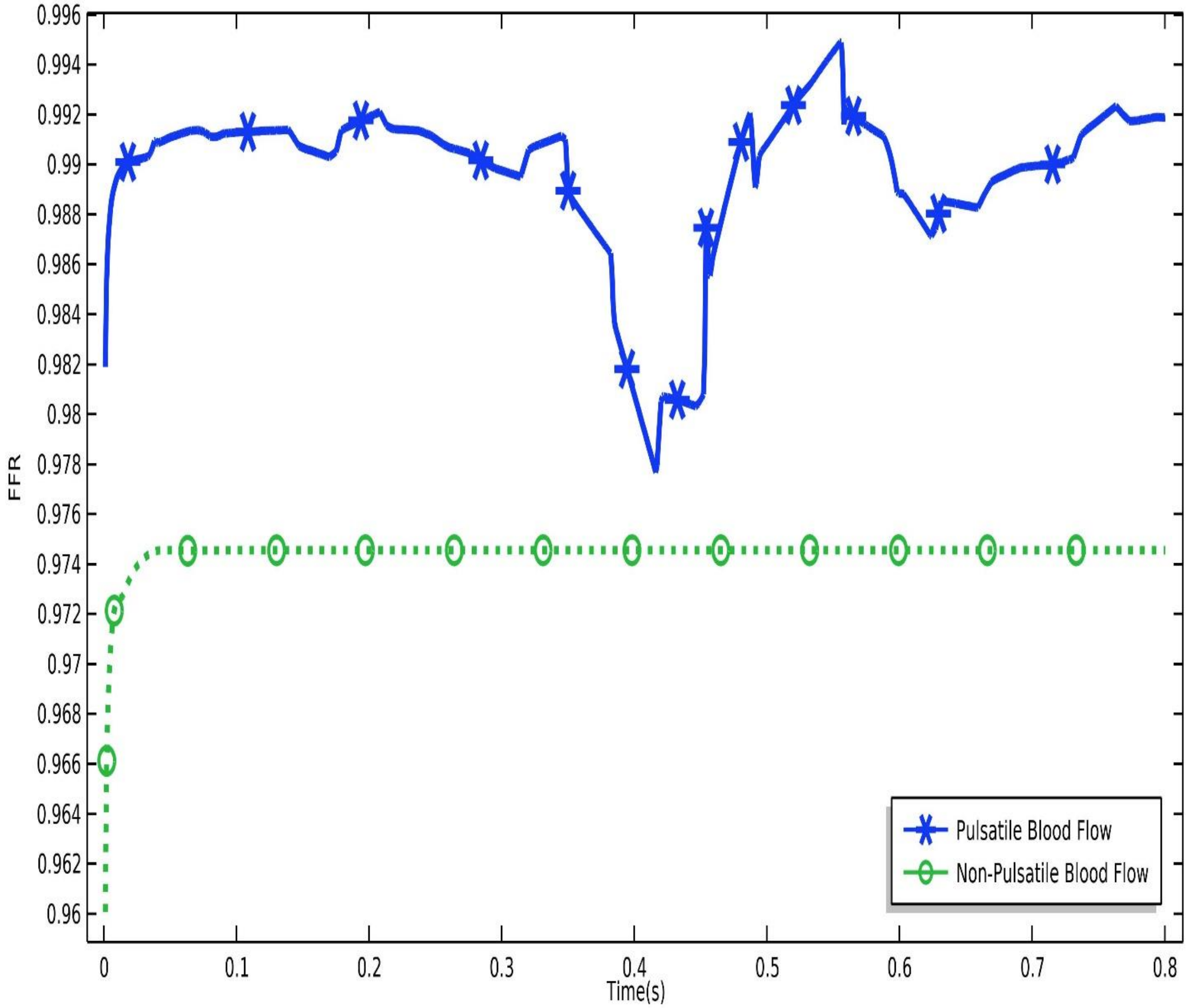

Figure 16: Comparison of FFR for pulsatile and non-pulsatile blood flows

The maximum values of FFR were obtained and then compared to invasive FFR results.

Table 4: Comparison of the FFR Results

FFR_{CT} for stationary non-pulsatile blood flow	0.97
FFR_{CT} for transient non-pulsatile blood flow	0.97
FFR_{CT} for transient pulsatile blood flow	0.99
FFR_{inv} with Adenosine	0.99

It is evident from the results that simulating pulsatile blood flow gave us more accurate results as compared to non-pulsatile blood flows.

CHAPTER 5. DISCUSSION

This chapter presents an insightful brief analysis of the applied methods and obtained results as explained in previous chapters. This chapter hast wo main sections. The first section contains a profound discussion on the methodology employed. The second section discusses the results and compares them with the results of other people.

5.1. On the Methods

The methodology developed for 3D geometric model belonging to a patient-specific is very much prone to the measurement and modelling errors. The capture of an accurate coronary artery and critical stenosis depends upon the ability of the interpretation of the DICOM CT images. Also, the quality of DICOM images is also a key parameter to develop a quality mesh.

Also, for the compatibility with COMSOL Multiphysics, no additional layers were fashioned from the vessel wall. For higher mesh refinement, the mesh inflation layers are desirable in the normal direction from the walls but without them, the viscous losses near the walls may be undervalued as these are of great importance for pulsatile flows.

The presented approach is incomplete regarding patient-specific limitations as only CTA images, HR and blood pressure has been taken form the patient. However, as our primary goal was to develop pulsatile flow for the assessment of FFR; the data obtained from the literature has made us able to calculate our required results very close to invasive results.

Vessel wall was modelled and assumed rigid. Malve et al shows that qualitative and quantitative errors are introduced by rigid walls for the calculation of wall-shear-stress (WSS). But Morris et al reported that there is no solid proof is available to support that compliance of the wall is necessary. Fluid-structure interface (FSI) is not entertained in this thesis. Also, the outlet pressure is assumed to be constant. Windkessel model (0D or 1D) may be introduced to calculate the outlet pressure from arterial tree but it is further based on some assumptions of resistances and compliances per se.

For non-pulsatile transient flows, the time period is set to 0.8 s as it was observed that it was enough for the results to converge but it is based on hit and trial method. Also, the time step for non-pulsatile flows was set to 0.001 s to observe when the results saturate.

For pulsatile flows, the time period for a single pulse is taken as 0.8 s which depends upon the heart rate of the patient.

We have used just two parameters to simulate blood i.e. density and viscosity which are constants and do not depend upon time.

5.2. On the Results

The results are solely dependent upon how accurate the geometrical model and how many patient-specific parameters had been used. The lack of knowledge and experience with radiology of the DICOM images may have caused geometrical artefacts. Geometrical disagreement is an inevitable challenge and misinterpretation of stenosis may have pronounced effects on the assessment of FFR.

Another main cause which may have affected the results is the approximation of hyperaemic flows in LAD. Many researchers have agreed that the right estimation of hyperaemic flow and coronary arterial geometry is the key to the successful assessment of FFR_{CT} as a diagnostic tool. These challenges are across the globe and despite of the limited extent of tailored patient-specific models, our results for presented methodology showed promising results.

The mesh study has enabled us to study the difference in results across the LAD domain. The mesh elements were not able to go beyond a certain limit although a coarser mesh produced more promising results which were closer to the invasive FFR. However, as more refined mesh is thought to be more realistic in results; we relied on the refined mesh.

The comparison of non-pulsatile steady and non-pulsatile transient results do not give any relevant information as viscosity and density both are not varying with time. Yet time step in transient simulations show when the results saturate to a steady state.

Although turbulence may occur in the coronary domain, yet these separated flows still can be laminar. The reason is that the Reynolds number for hemodynamically flows are much less than 2200 which is a typical Reynolds number for transition from laminar to turbulence in flows.

As viscosity and density are constants and do not depend upon time; transient simulations for non-pulsatile flows do not give us any further information.

The study also suggests that as the vessel gets narrowed at the outlet, the velocity keeps increasing for non-Pulsatile flows while using a pulsatile flow, the velocity remains in a range which goes in hand with the theory of pulsatile flows as shown in the figure.

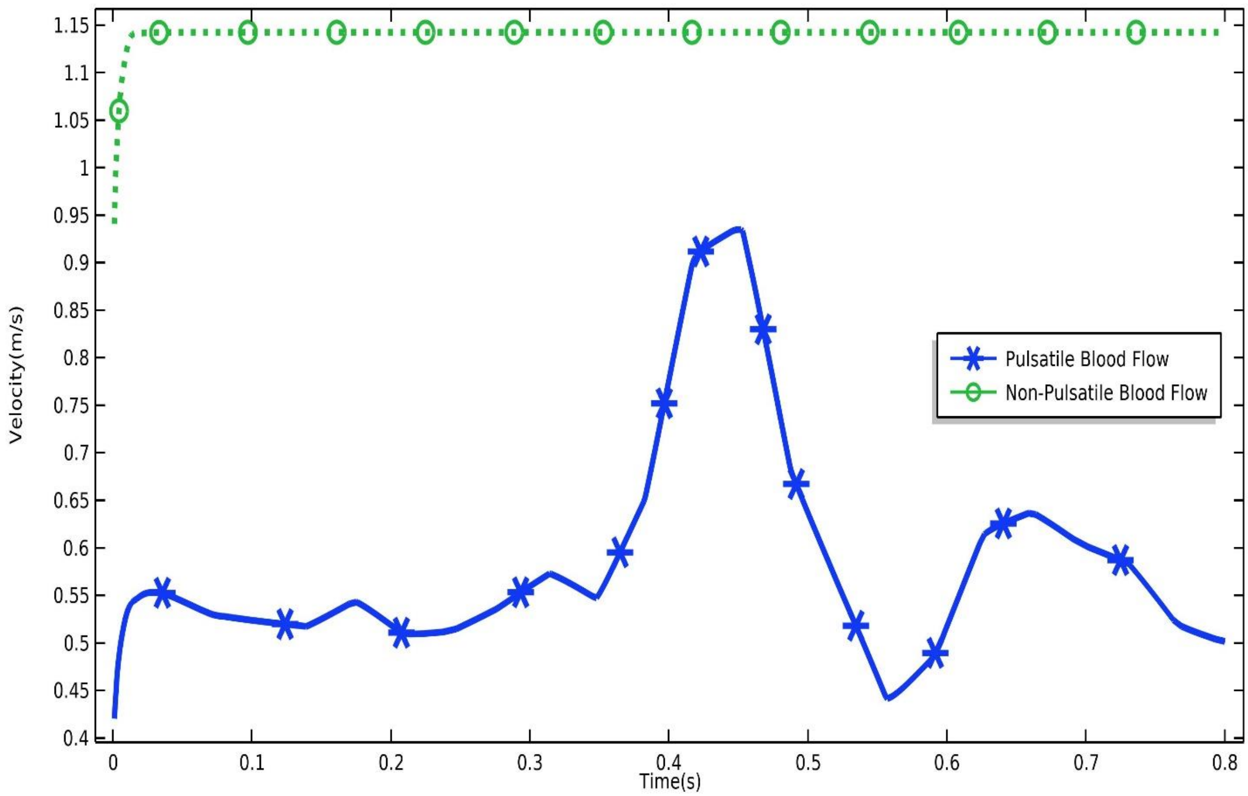

Using pulsatile flow, we have obtained our results closest to invasive FFR.

CHAPTER 6. CONCLUDING REMARKS

This chapter contains key points from the work explained in previous chapters. First section summarises the work done in this thesis. Second section discusses the concluding remarks. Finally, third section discusses the limitations of this project and suggests the directions for future work.

6.1. Summary of the project

The presented work in this thesis is related to the CFD simulation of the coronary blood flow for a patient-based coronary artery (Left Anterior Descending) for the calculation of fractional flow reserve (FFR) non-invasively. The patient-specific model of LAD was constructed using CT Angiography images data of the patient using Mimics Materialise 21. The blood had been modelled as non-Newtonian. Steady and Transient simulations were conducted for a non-pulsatile blood flow and Transient simulations for a pulsatile blood flow using COMSOL Multiphysics 5.4. The results obtained from CFD simulations were analysed and compared with invasive FFR measurements which led to the discussion on applied methods.

6.2. Conclusion

The computational models developed and applied in this thesis shows promising results. It resembles to the physiological coronary flows developed by other people and in arrangement with the latest models for simulations. The difference between invasive FFR and FFR_{CT} is negligible in case of a pulsatile flow as compared to the non-pulsatile steady state and transient flows. The presented methodology is sufficient for comparison of invasive FFR and FFR_{CT} as the simulation of pulsatile flow for the assessment of FFR_{CT} introduce insignificant errors based on the finding of this work.

6.3. Limitations

This study only investigates the coronary blood flow in LAD only. The reason is that the patient had only been diagnosed for FFR in LAD only. A complete investigation of coronary arterial tree can be also be done with a high-quality CTA data.

The data had been obtained only from one patient which limits the extent to the study and the obtained results with the span of FFR. Also, only the CTA data, blood pressure and pulsatile flow are obtained from the patient. The fluid-structure interaction had not been accounted in the present work.

6.4. Suggestions for the future work

The computational calculation of FFR is facing many challenges. One of them is that FFR is a costly procedure and not essential for every patient. Following are the suggestions to improve the outcome of the results for the subsequent work:

- A pilot study can be developed for a larger group of patients for a broader span of FFR in order to encourage the outcome of the results for the presented methodology
- The segmentation process can be automated
- Coronary flow rate and velocity can be obtained using Doppler ultrasound for a more precise study of the patient specific model
- The quality of the results can be improved using a high-quality CT Angiography images with better resolution.
- Windekessel Model can be used to calculate arterial pressure at the outlet of the coronary arteries

REFERENCES

[1] D. Mozaffarian *et al.*, "Heart disease and stroke statistics-2016 update a report from the American Heart Association," vol. 133, no. 4, pp. e38-e48, 2016.

[2] "World Health Organization: Health statistics and information systems."

[3] W. F. Fearon, A. C. Yeung, D. P. Lee, P. G. Yock, and P. A. J. A. h. j. Heidenreich, "Cost-effectiveness of measuring fractional flow reserve to guide coronary interventions," vol. 145, no. 5, pp. 882-887, 2003.

[4] M. A. Hlatky, A. Saxena, B. K. Koo, A. Erglis, C. K. Zarins, and J. K. J. C. c. Min, "Projected Costs and Consequences of Computed Tomography-Determined Fractional Flow Reserve," vol. 36, no. 12, pp. 743-748, 2013.

[5] J. K. Min *et al.*, "Noninvasive fractional flow reserve derived from coronary CT angiography: clinical data and scientific principles," vol. 8, no. 10, pp. 1209-1222, 2015.

[6] B. De Bruyne *et al.*, "Fractional flow reserve–guided PCI versus medical therapy in stable coronary disease," vol. 367, no. 11, pp. 991-1001, 2012.

[7] N. H. Pijls *et al.*, "Measurement of fractional flow reserve to assess the functional severity of coronary-artery stenoses," vol. 334, no. 26, pp. 1703-1708, 1996.

[8] P. S. Douglas *et al.*, "Clinical outcomes of fractional flow reserve by computed tomographic angiography-guided diagnostic strategies vs. usual care in patients with suspected coronary artery disease: the prospective longitudinal trial of FFRCT: outcome and resource impacts study," vol. 36, no. 47, pp. 3359-3367, 2015.

[9] *A Normal & Stenosed Artery*. Available: http://www.columbianeurology.org/neurology/staywell/document.php?id=35842

[10] *Anatomy of coronary arteries*. Available: https://upload.wikimedia.org/wikipedia/commons/9/93/Blausen_0256_CoronaryArteries_02.png

[11] (Measurement of Invasive FFR). Available: https://files.radcliffecardiology.com/s3fs-public/image-gallery/judefig2_1.gif

[12] C. A. Taylor, T. A. Fonte, and J. K. J. J. o. t. A. C. o. C. Min, "Computational fluid dynamics applied to cardiac computed tomography for noninvasive quantification of fractional flow reserve: scientific basis," vol. 61, no. 22, pp. 2233-2241, 2013.

[13] B. L. Nørgaard *et al.*, "Diagnostic performance of noninvasive fractional flow reserve derived from coronary computed tomography angiography in suspected coronary artery disease: the NXT trial (Analysis of Coronary Blood Flow Using CT Angiography: Next Steps)," vol. 63, no. 12, pp. 1145-1155, 2014.

[14] W. F. Fearon *et al.*, "Accuracy of fractional flow reserve derived from coronary angiography," vol. 139, no. 4, pp. 477-484, 2019.

[15] J.-M. Zhang *et al.*, "Simplified models of non-invasive fractional flow reserve based on CT images," vol. 11, no. 5, 2016.

[16] P. D. Morris *et al.*, "Virtual fractional flow reserve from coronary angiography: modeling the significance of coronary lesions: results from the VIRTU-1 (VIRTUal Fractional Flow Reserve From Coronary Angiography) study," vol. 6, no. 2, pp. 149-157, 2013.

[17] Y. Huo, M. Svendsen, J. S. Choy, Z.-D. Zhang, and G. S. J. J. o. T. R. S. I. Kassab, "A validated predictive model of coronary fractional flow reserve," vol. 9, no. 71, pp. 1325-1338, 2012.
[18] R. E. Mates, R. L. Gupta, A. C. Bell, and F. J. J. C. r. Klocke, "Fluid dynamics of coronary artery stenosis," vol. 42, no. 1, pp. 152-162, 1978.
[19] W. F. Fearon, P. A. Tonino, B. De Bruyne, U. Siebert, N. H. Pijls, and F. S. I. J. A. h. journal, "Rationale and design of the fractional flow reserve versus angiography for multivessel evaluation (FAME) study," vol. 154, no. 4, pp. 632-636, 2007.
[20] C. A. Bulant, P. J. Blanco, G. M. Talou, C. G. Bezerra, P. A. Lemos, and R. A. J. J. o. b. Feijóo, "A head-to-head comparison between CT-and IVUS-derived coronary blood flow models," vol. 51, pp. 65-76, 2017.
[21] M. Zamir, *The physics of coronary blood flow*. Springer Science & Business Media, 2006.
[22] B. R. Weil and J. M. Canty, "Coronary Blood Flow and Myocardial Ischemia," in *Essential Cardiology*: Springer, 2013, pp. 387-403.
[23] S. Aamodt, "Computational Diagnosis of Coronary Artery Disease-A comparison of steady and transient blood flow simulations for FFR," NTNU, 2017.
[24] *Blood Flow during Diastole & Systole*. Available: https://www.thoughtco.com/thmb/F1x6_Hthein9tc4AZAYCiNJDWww=/768x0/filters:no_upscale():max_bytes(150000):strip_icc():format(webp)/cardiac_cycle-597a5d8168e1a200115e5937.jpg
[25] N. Westerhof, N. Stergiopulos, and M. J. N. Y. Noble, "Snapshots of hemodynamics: an aid for clinical research and graduate education. Springer Verlag," 2010.
[26] D. F. Young and F. Y. J. J. o. b. Tsai, "Flow characteristics in models of arterial stenoses—I. Steady flow," vol. 6, no. 4, pp. 395-410, 1973.
[27] S. Sakamoto *et al.*, "Relation of distribution of coronary blood flow volume to coronary artery dominance," vol. 111, no. 10, pp. 1420-1424, 2013.
[28] A. R. Jayaweera *et al.*, "Role of capillaries in determining CBF reserve: new insights using myocardial contrast echocardiography," vol. 277, no. 6, pp. H2363-H2372, 1999.
[29] R. F. Wilson, K. Wyche, B. V. Christensen, S. Zimmer, and D. D. J. C. Laxson, "Effects of adenosine on human coronary arterial circulation," vol. 82, no. 5, pp. 1595-1606, 1990.
[30] E. O. Ofili, A. J. Labovitz, and M. J. J. T. A. j. o. c. Kern, "Coronary flow velocity dynamics in normal and diseased arteries," vol. 71, no. 14, pp. D3-D9, 1993.
[31] J. D. Rossen, J. E. Quillen, J. A. G. Lopez, R. G. Stenberg, C. L. Talman, and M. D. J. J. o. t. A. C. o. C. Winniford, "Comparison of coronary vasodilation with intravenous dipyridamole and adenosine," vol. 18, no. 2, pp. 485-491, 1991.
[32] C. L. J. T. m. p. p. Fefferman, "Existence and smoothness of the Navier-Stokes equation," vol. 57, p. 67, 2006.
[33] J. Donea and A. Huerta, *Finite element methods for flow problems*. John Wiley & Sons, 2003.
[34] W. B. Zimmerman, *Multiphysics modeling with finite element methods*. World Scientific Publishing Company, 2006.
[35] L. G. Leal, *Advanced transport phenomena: fluid mechanics and convective transport processes*. Cambridge University Press, 2007.
[36] J. F. Wendt, *Computational fluid dynamics: an introduction*. Springer Science & Business Media, 2008.

[37] H. M. Nydal and J. K. Kjernlie, "Closing the Gap between Reality and CFD Simulations of FFR with Techniques to Quantify and Reduce Uncertainty of Predictions," NTNU, 2016.

[38] P. D. Morris, F. N. van de Vosse, P. V. Lawford, D. R. Hose, and J. P. J. J. C. I. Gunn, "“Virtual”(computed) fractional flow reserve: current challenges and limitations," vol. 8, no. 8, pp. 1009-1017, 2015.

[39] E. Holte, J. Vegsundvåg, K. Hegbom, T. Hole, and R. J. J. o. t. A. S. o. E. Wiseth, "Transthoracic Doppler echocardiography for detection of stenoses in the left coronary artery by use of poststenotic coronary flow profiles: a comparison with quantitative coronary angiography and coronary flow reserve," vol. 26, no. 1, pp. 77-85, 2013.